IMPLEMENTATION OF FUZZY LOGIC IN POWER SYSTEM STABILIZER TO IMPROVE SYSTEM DAMPING

A DISSERTATION SUBMITTED IN PARTIAL FULFILLMENT OF THE REQUIREMENTS FOR THE AWARD OF THE DEGREE OF

MASTER OF ENGINEERING
IN
CONTROL & INSTRUMENTATION

BY

VIKAS ANAND

UNDER THE ESTEEMED GUIDANCE

OF

Mr. RAM BHAGAT

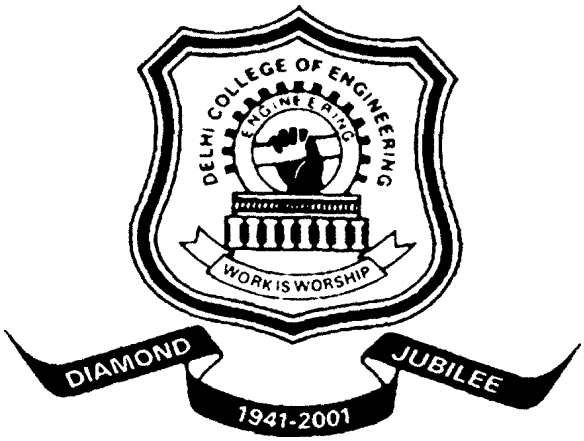

DEPARTMENT OF ELECTRICAL ENGINEERING
DELHI COLLEGE OF ENGINEERING
UNIVERSITY OF DELHI
2005-2006

CERTIFICATE

It is certified that Vikas Anand, Roll No.8668, student of M.E, Control and Instrumentation, Department of Electrical Engineering, Delhi College of Engineering, has submitted the dissertation entitled **"Implementation of Fuzzy Logic in Power system stabilizer to improve system damping"**, under my guidance towards partial fulfillment of the requirements for the award of the degree of Master of Engineering (Control & Instrumentation Engineering).

This dissertation is a bonafide record of project work carried out by him under my guidance and supervision. His work is found to be excellent during the course of the project.

Dated:

(Mr. Ram Bhagat)
RAM BHAGAT
Lecturer
Department of Electrical Engineering
Delhi College of Engineering
Delhi- 110042.

ACKNOWLEDGEMENT

I feel honored in expressing my profound sense of gratitude and indebtedness to Mr. Ram Bhagat, Lecturer, Department of Electrical Engineering, Delhi college of Engineering, Delhi for his expert guidance, meticulous efforts, constructive criticism, inspiring encouragement, unflinching support and invaluable co-operation which enabled me to enrich my knowledge and reproduce it in the present form.

I also like to extend my gratefulness to Prof. Parmod Kumar, HOD Dept. of Electrical Engineering, Delhi college of Engineering, for his perpetual encouragement, generous help and inspiring guidance.

I would like to extend my sincere appreciation to my friend Mr**.** Shabir Masood for providing me all sources and reviewing this report and providing valuable comments and thoughtful criticism, which have resulted in an improved version.

There are times in a project when the clock beats our time and we run out of energy, wishing to finish it once and forever. My parents made me endure such times with their unconditional support and love.

Dated:

Vikas Anand

Roll No. 8668

ABSTRACT

The use of power system stabilizers has become very common in operation of large electric power systems. However, it was very difficult to design a stabilizer that could present good performance in all operating points of electric power systems. In an attempt to cover a wide range of operating conditions, Fuzzy logic control has been suggested as a possible solution to overcome this problem, by using linguist information and avoiding a complex system mathematical model.

In this thesis, a systematic approach to fuzzy logic control design is proposed. This paper presents a study of fuzzy logic power system stabilizer for stability enhancement of a single machine infinite bus system. In order to accomplish the stability enhancement, speed deviation $\Delta\omega$ and acceleration $\Delta\dot{\omega}$ of the rotor synchronous generator were taken as the inputs to the fuzzy logic controller. These variables take significant effects on damping the generator shaft mechanical oscillations. The stabilizing signals were computed using the fuzzy membership function depending on these variables. Simulink Block Design and Matlab-7 is utilized in implementing the study. The performance of the fuzzy logic power system stabilizer iss compared with the conventional power system stabilizer and without power system stabilizer. Also the scaling parameters of proposed fuzzy logic controller are determined offline using genetic algorithm.

.

CONTENTS

Page No.

LIST OF FIGURES

LIST OF TABLES

LIST OF SYMBOLS

SYMBOL	QUANTITY
δ	Rotor Angle
ω_r	Rated Speed (in electrical rad/s = $2\pi f$
$\Delta\delta$	Rotor Angle Deviation
$\Delta\omega_r$	Speed Deviation (in p.u.) $= \left((\omega_r - \omega_o) / \omega_o \right)$
$\Delta\omega$	Speed deviation (Input to fuzzy logic Controller)
$\Delta\dot{\omega}$	Deviation in angular acceleration
ω_n	Undamped Natural Frequency (in rad/s)
ΔT_m	Deviation in Mechanical Torque
ξ	Damping Ratio
ψ_{fd}	Field Circuit Flux Linkage
ψ_d , ψ_q	d-axis and q-axis Flux Linkage
L'_{ads} , L'_{aqs}	Saturated values of Transient Inductances
ψ_{ad} , ψ_{aq}	Air Gap Flux Linkage
A_{sat} , B_{sat}	Constants defining Saturation Characteristics of Machine
E_B	Infinite Bus Voltage (in p.u)
E_t	Generator Terminal Voltage.

e_d , e_d	d-axis and q-axis component of E_t
E_{fd}	Exciter Output Voltage
FPSS	Fuzzy Logic Power System Stabilizer
GFPSS	Genetic algorithm fuzzy logic power system stabilizer
H	Inertial Constant (in MW-s/MVA)
I	Line Current (in p.u.)
I_d , I_q	d-axis and q-axis components of line current
I_{fd}	Field Current
J	Combined Moment of Inertia of generator and turbine (in Kg-m^2)
K_1,K_2,K_3,K_4,K_5 ,K_6	K-Constants of Phillips Heffron Model
K_A	Exciter Gain
K_D	Damping Torque Coefficient (in p.u torque/ p.u speed deviation)
K_S	Synchronizing Torque Coefficient (in p.u. torque/rad.)
$K_{sd(incr)}$, $K_{sq(incr)}$	Incremental Saturation Factor
K_{STAB}	Stabilizer Gain
L_l	Leakage Inductance
L_{fd}	Field Winding Inductance
L_{ad}, L_{aq}	d-axis and q-axis Mutual Inductance
L_{ads}, L_{aqs}	Saturated values of d-axis and q-axis Mutual Inductance
P	Active Power (in p.u.)
PSS	Power System Stabilizer
p	Differential Coefficient
P_e	Air Gap Power (in p.u.)
p_f	Number of field Poles

Q	Reactive Power (in p.u.)
R_a	Armature Resistance per Phase (in p.u.)
R_E	Transmission Line Resistance (in p.u.)
R_{fd}	Field Circuit Resistance
R_T	Total Resistance (in p.u.)
s	Laplace Operator
T_1, T_2	Phase Compensation Time Constant
T_3	Time Constant of Field Circuit
T_a	Accelerating torque (in N-m)
T_e	Electromagnetic Torque (in N-m)
T_m	Mechanical Torque (in N-m)
T_W	Time Constant of Wash out block
$\overline{T}_m$	Mechanical Torque (in p.u.)
$\overline{T}_e$	Electromagnetic Torque (in p.u.)
X'_d	Transient Reactance of Generator
X_E	Transmission Line Reactance (in p.u.)
X_T	Total Reactance (in p.u)

CHAPTER 1

INTRODUCTION

Excitation control is well known as one of the effective means to enhance the overall stability of electric power systems. Conventional power system stabilizers have been used to provide the desired system performance under condition that requires stabilization. Stability of synchronous generator depends on a number of factors such as the setting of automatic voltage regulator (AVR). Many generators are designed with high gain, fast acting AVR's to enhance large scale stability to hold the generator in synchronism with the power system during large transient fault condition. But with the high gain of excitation systems, it can decrease the damping torque of the generator. A supplementary excitation controller referred to as power system stabilizers (PSS) have been added to synchronous generators to counteract the effect of high gain AVR's and other sources of negative damping.

To improve damping the stabilizer must produce a component of electrical torque on the rotor which is in phase with speed variations

The application of a power system stabilizer (PSS) is to generate a supplementary stabilizing signal, which is applied to excitation system to control loop of the generating unit to produce a positive damping the most widely used conventional power system stabilizer is lead-lag PSS where the gain settings are fixed at certain value which are determined under particular operating conditions to result in optimal performance for the specific condition. However, they give poor performance under different synchronous generator loading conditions.

Limitations of fixed parameters of conventional PSS have been reduced by using fuzzy logic controllers. Unlike the classical logic approach, which requires a deep understanding of a system, exact equations and precise numeric values, fuzzy logic incorporates an alternative way of thinking which allows one to model complex systems using a higher level of abstraction originated from accumulated knowledge and experience. Fuzzy logic allows one to express the knowledge with subjective concepts such as very tall, too small, moderate and slightly deviated, which are mapped on to numeric ranges.

The objective of the thesis is to study and design the fuzzy logic power system stabilizer used for small signal stability analysis. It is based on the implementation of fuzzy logic technique to power system stabilizer to improve system damping. The effectiveness of the fuzzy logic PSS in a single machine infinite bus is demonstrated by a Simulink model. (MATLAB 7 software package). The performance of fuzzy logic PSS is compared with the conventional PSS and without PSS. The time-domain simulation performed on the test system will be employed to study the small signal stability. Discrete simulation is also performed using Matlab code.

1.1 EFFECT OF EXCITATION CONTROL

It is worth while to understand the effect of the excitation system on the dynamic performance of power system. To begin with, the Automatic Voltage Regulator (AVR) and the generator field dynamics introduces phase lag so that the resulting torque is out of phase with both rotor angle and speed deviations. S positive synchronizing torque and a negative damping torque often result, which can cancel the small inherent positive damping torque available, leading to instability.

Present day excitation systems predominantly constitute fast acting AVRs. A high response exciter is beneficial in increasing the synchronizing torque, thus enhancing the transient stability. However it produces negative damping especially at high values of

external system reactance and high generator outputs, thus affecting the small signal stability. For inter area power transfer, in the control jargon it can be stated that the frequency and damping ratios of the oscillation mode drops, as the tie-line impedance or the power flow is increased.

1.2 POWER SYSTEM STABILIZER

Generator excitation controls have been installed and made faster to improve stability. Power system stabilizers have been added to the excitation systems to improve oscillatory instability it is used to provide a supplementary signal to the excitation system. The basic function of the power system stabilizer is to extend the stability limit by modulating generator excitation to provide positive damping torque to power swing modes.

A typical power system stabilizer consists of a phase compensation stage, a signal washout stage and a gain block. To provide damping, a PSS must provide a component of electrical torque on the rotor in phase with the speed deviations. Power system stabilizer input signals includes generator speed, frequency and power. For any input signal, the transfer function of the PSS must compensate for the gain and phase characteristics of the excitation system, the generator and the power system. These collectively determine the transfer function from the stabilizer output to the component of electrical torque which can be modulated via excitation control.

The PSS, while damping the rotor oscillations, can cause instability of the turbine generator shaft torsional modes. Selection of shaft speed pick-up location and torsional notch filters are used to attenuate the torsional mode frequency signals. The PSS gain and torsional filter however, adversely affects the exciter mode damping ratio. The use of accelerating power as input signal for the PSS attenuates the shaft torsional modes inherently, and mitigates the requirements of the filtering in the main stabilizing path

1.3 FUZZY LOGIC BASED POWER SYSTEM STABILIZER

Power system stabilizer give poor performance under different synchronous generator loading conditions hence the need for fuzzy logic power system stabilizer arises. In order to accomplish a satisfactory damping characteristic over a wide range of operating points, speed deviation ($\Delta\omega$) and acceleration $\left(\Delta\dot{\omega}\right)$ of a synchronous generator were taken as the input signals to the fuzzy controller. It is well known that these variables have significant effects on damping the generators shaft mechanical oscillations. A modification of the terminal voltage feedback signal to the excitation system as a function of the accelerating power on the unit is also used to enhance the stability of the system. The stabilizing signals are computed using the standard fuzzy membership function depending on these variables. The performance of the proposed fuzzy logic power system stabilizer is compared to PSS and its effectiveness is demonstrated by a detailed digital computer simulation of a single machine infinite bus system.

CHAPTER 2

LITERATURE REVIEW

2.1 AN OVERVIEW

In early days, many power generating plants were equipped with continuously acting automatic voltage regulators. As the power generated increase and high response exciters come into picture with the use automatic voltage regulators grew it became apparent that the high performance of these voltage regulators had a destabilizing effect on the power system. Power oscillations of small magnitude and low frequency often persisted for long periods of time. In some cases, this presented a limitation on the amount of power able to be transmitted within the system. Power system stabilizers were developed to aid in damping of these power oscillations by modulating the excitation supplied to the synchronous machine.

The power system stabilizer normally consists of a phase-lead compensation blocks, a signal washout block, and a gain block. The input signal to the stabilizer is the equivalent rotor speed deviation. But due to constant stabilizer gain and the complexity of system modeling under different operating conditions calls for new technology to be introduced in damping of small signal oscillation of the system giving origin new type of linguistic based power system stabilizer called fuzzy logic based power system stabilizer. The fuzzy logic based power system stabilizer removes most of the shortcomings of the conventional power system stabilizer before this fuzzy logic stabilizer auto tuned power system stabilizer is also consider under this thesis to explain some of the generalized aspects of power system stabilizer.

2.2 THEORETICAL BACKGROUND

Small signal stability is defined as the ability of the power system to remain stable in the presence of small disturbances. These disturbances could be minor variations in load or generation on the system. If sufficient damping torque doesn't exist, the result can be rotor angle oscillations of increasing amplitude. Generators connected to the grid utilizing high gain automatic voltage regulators can experience insufficient damping to system oscillations.

To further understand the difference between the good effect of high performance excitation systems and the side-effect of reduced damping torque, consider the equation:

$$\Delta T_e = T_S \Delta\delta + T_D \Delta\omega$$

Above equation break electrical torque ΔT_e into the two components of synchronizing torque T_S and damping torque T_D. The synchronizing torque increases the pull between rotor and stator flux, decreasing the angle δ, and reducing the risk of pulling out of step. The damping torque, on the other hand, results from the phase lag or lead of the excitation current. Like the timing of pushes to a swing, the excitation current acting to improve synchronizing torque normally is time delayed by the characteristics of the excitation system, the time delay of the alternator field, and the time delay of the exciter field (if used). These time delays cause the effect of a high initial response excitation system to cause negative damping, resulting in loss of small-signal stability. Loss of small-signal stability results in one or more of the types of oscillations listed below:

Three types of oscillations that have been experienced with large interconnected generators and transmission networks include:

Inter-unit Oscillations - These oscillations involve typically two or more synchronous machines at a power plant or nearby power plants. The machines swing against each other, with the frequency of the power oscillation ranging between 1.5 to 3 Hz.

Local Mode Oscillations- These oscillations generally involve one or more synchronous machines at a power station swinging together against a comparatively large power system or load center. The frequency of oscillation is in the range of 0.7 Hertz to 2 Hertz. These oscillations become troublesome when the plant is at high load with a high reactance transmission system.

Inter-area Oscillations- These oscillations usually involve combinations of many machines on one part of a power system swinging against machines on another part of the power system. Inter-area oscillations are normally in the frequency range of less than 0.5 Hz.

2.3 RECENT WORK

Fast excitation systems were introduced earlier to recognize the change in terminal voltage due to various causes and to remove it. These fast excitation system recognize a change in voltage due to load change up to 10 times faster than older excitation systems. Thus, small oscillations of the unit cause the excitation system to correct immediately. Because of the high inductance in the generator field winding however, the field current rate of change is limited. This introduces considerable "lag" in the control function. Thus from the time of recognition of a desired excitation change to its partial fulfillment, there is an unavoidable time delay. During this delay time, the state of the oscillating system will change, causing a new excitation adjustment to be started. The net result is the excitation system tends to lag behind the need for a change, aiding the inherent oscillatory behavior of the generators interconnected by transmission lines.

One solution to improve the dynamic performance of this system and large-scale systems in general would be to add more parallel transmission lines to reduce the reactance between the generator and load center. This solution is well known, but usually it is not acceptable due to the high cost of building transmission lines. An alternative solution adds a power system stabilizer (PSS) that acts through the voltage regulator. Working together, the excitation output is modulated to provide positive damping torque to the system.

CHAPTER 3

SYSTEM MODELLING

A general system configuration for the synchronous machine connected to the large system is shown in figure 3.1(a). This general system is used for the study of small signal stability study.

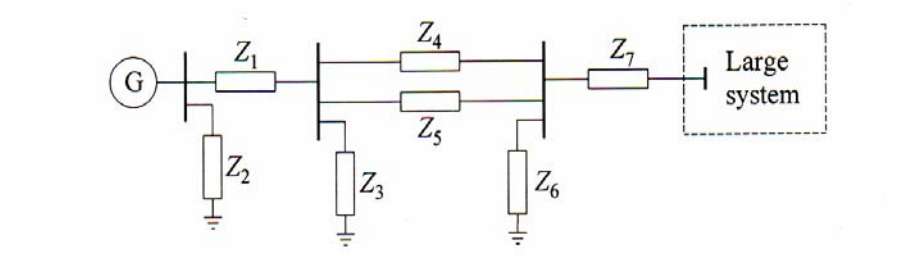

Figure 3.1: General configuration of single machine connected to a large system through transmission line

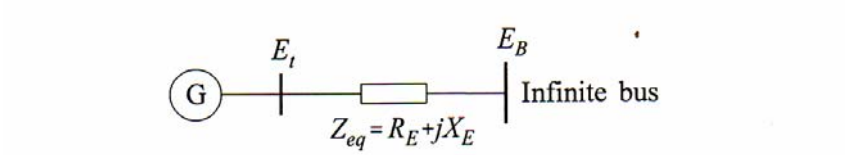

Figure 3.2: Equivalent circuit

The general system configuration can be reduced to the Thevenin's equivalent circuit shown in figure 3.2

For any given system condition, the magnitude of the infinite bus voltage E_B remain constant when machine is perturbed.

3.1 CLASSICAL MODEL REPRESENTATION

With the generator represented by the classical model and all resistances neglected, the system representation is as shown in Figure 3.3. Here E' is the voltage behind Xd'. Its magnitude is assumed to remain constant at the pre-disturbance value. Let S be the angle by which .E.' leads the infinite bus _voltage E_B As the rotor oscillates during a disturbance, δ changes.

With E' as reference phasor,

$$\tilde{I}_t = \frac{E'\angle 0^\circ - E_B\angle -\delta}{jX_T} = \frac{E'\text{-}E_B(\cos\delta - j\sin\delta)}{jX_T} \qquad (3.1)$$

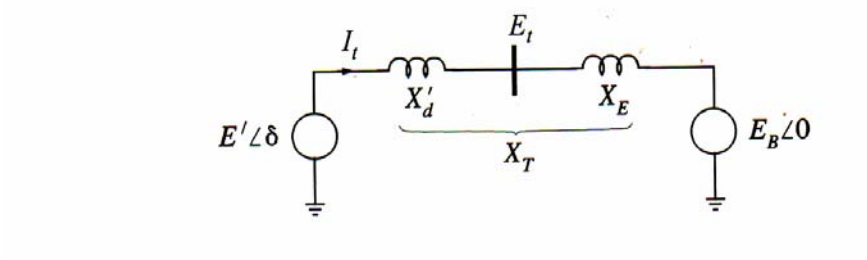

Figure 3.3: classical model of generator

The complex power behind Xd' is given by:

$$= \frac{E'E_B\sin\delta}{X_T} + j\frac{E'(E'\text{-}E_B\cos\delta)}{X_T} \qquad (3.2)$$

With stator resistance neglected, the air-gap power (P_e) is equal to the terminal power (P). In per unit, the air-gap torque is equal to the air-gap power. Hence

$$T_e = P = \frac{E'E_B}{X_T}\sin\delta \qquad (3.3)$$

Linearizing about an initial operating condition represented by $\delta=\delta_o$ yields

$$\Delta T_e = \frac{\partial T_e}{\partial \delta}\Delta\delta = \frac{E'E_B}{X_T}\cos\,\delta_o(\Delta\delta) \tag{3.4}$$

The equations of motion in per unit are:

$$p\Delta\omega_r = \frac{1}{2H}(T_M - T_e - K_D\Delta\omega_r) \tag{3.5}$$

$$p\delta = \omega_o\Delta\omega_r \tag{3.6}$$

Linearizing Equation 3.5 and substituting for ΔT, given by Equation 3.4, we obtain:

$$p\Delta\omega_r = \frac{1}{2H}(\Delta T_M - K_s\Delta\delta - K_D\Delta\omega_r) \tag{3.7}$$

$$K_s = \left(\frac{E'E_E}{X_T}\right)\cos\delta_o \tag{3.8}$$

Linearizing Equation 3.6, we have

$$p\Delta\delta = \omega_o\Delta\omega_r \tag{3.9}$$

Writing equation 3.5 and 3.6 in matrix form we obtain

$$\frac{d}{dt}\begin{bmatrix} -K_D & -\frac{K_s}{2H} \\ \omega_o & 0 \end{bmatrix}\begin{bmatrix}\Delta\omega \\ \Delta\delta\end{bmatrix} + \begin{bmatrix}\frac{1}{2H} \\ 0\end{bmatrix}\Delta T_m \tag{3.10}$$

This is of the form $\dot{x} = Ax + bu$. The elements of the state matrix A are seen to be dependent on the system parameters K_D, H, X_T, and the initial operating condition

represented by the value of E' and δ_o. The Block diagram representation shown in figure 3.4 can be used to describe the small-signal performance.

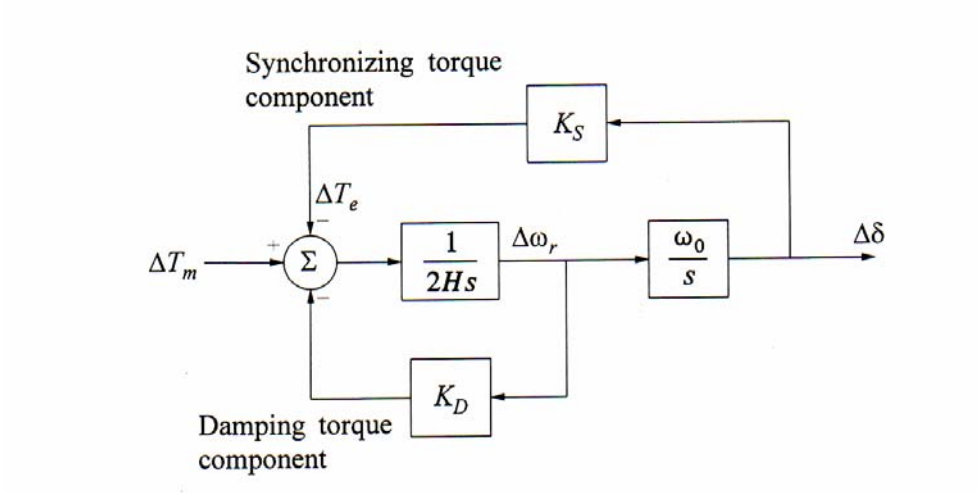

Figure 3.4 : Block diagram of a single-machine infinite bus system with classical generator model

From the block diagram we have:

$$\Delta\delta = \frac{\omega_o}{s}\left[\frac{1}{2Hs}\left(-K_S\Delta\delta - K_D\Delta\omega_r + \Delta T_m\right)\right]$$

$$= \frac{\omega_o}{s}\left[\frac{1}{2Hs}\left(-K_S\Delta\delta - K_D s\frac{\Delta\delta}{\omega_o} + \Delta T_m\right)\right] \qquad (3.11)$$

Solving the block diagram we get the characteristic equation:

$$s^2 + \frac{K_D}{2H}s + \frac{K_s\omega_o}{2H} = 0 \qquad (3.12)$$

Comparing it with general form we get

The undamped natural frequency is:

$$\omega_n = \sqrt{K_s\frac{\omega_o}{2H}} \quad \text{rad/s} \qquad (3.13)$$

And the damping ratio is

$$\xi = \frac{1}{2}\frac{K_D}{\sqrt{K_S 2H\omega_o}} \tag{3.14}$$

3.2 EFFECT OF FIELD CIRCUIT DYNAMICS

Under field circuit dynamics we will develop the state space model of the system by first reducing the synchronous machine equations to an appropriate form and then combining them with the network equations.

The acceleration equation of the generator model is given by:

$$p\Delta\omega_r = \frac{1}{2H}\left(T_m - T_e - K_D\Delta\omega_r\right) \tag{3.15}$$

$$p\delta = \omega_o\Delta\omega_r \tag{3.16}$$

Synchronous generator field circuit dynamic equations are given by:

$$p\psi_{fd} = \omega_o\left(e_{fd} - R_{fd}i_{fd}\right)$$

$$= \omega_o\frac{R_{fd}}{L_{adu}}E_{fd} - \omega_o R_{fd}i_{fd} \tag{3.17}$$

Where E_{fd} is the exciter output voltage.

The equivalent circuits relating the machine flux linkages and currents are shown in figure (3.5)

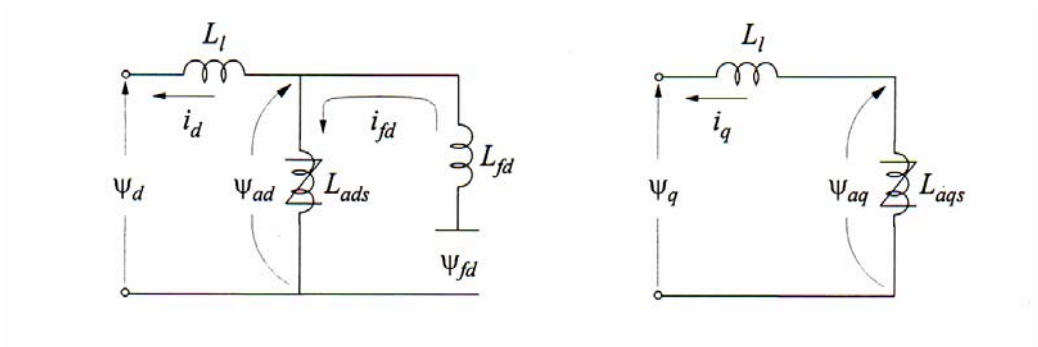

Figure 3.5: Equivalent circuits relating the machine flux linkage and current

The stator and rotor flux linkage are given by:

$$\psi_d = -L_l i_d + L_{ads}\left(-i_d + i_{fd}\right)$$

$$= -L_l i_d + \psi_{ad} \tag{3.18}$$

$$\psi_q = -L_l i_q + L_{aqs}\left(-i_q\right)$$

$$= -L_l i_q + \psi_{aq} \tag{3.19}$$

$$\psi_{fd} = L_{ads}\left(-i_d + i_{fd}\right) + L_{fd} i_{fd}$$

$$= \psi_{ad} + L_{fd} i_{fd} \tag{3.20}$$

From equation 3.20, the field circuit may be expressed as:

$$i_{fd} = \frac{\psi_{fd} - \psi_{ad}}{L_{fd}} \tag{3.21}$$

The d-axis mutual flux linkage can be written in terms of ψ_{fd} and i_d as follows:

$$\psi_{ad} = -L_{ads} i_d + L_{ads} i_{fd}$$

$$\begin{aligned} &= -L_{ads} i_d + \frac{L_{ads}}{L_{fd}} \left(\psi_{fd} - \psi_{ad} \right) \\ &= L'_{ads} \left(-i_d + \frac{\psi_{fd}}{L_{fd}} \right) \end{aligned} \tag{3.22}$$

Where

$$L'_{ads} = \frac{1}{\frac{1}{Lads} + \frac{1}{L_{fd}}}$$

Since there are no rotor circuits considered in the q-axis, the mutual flux linkage is given by:

$$\psi_{aq} = -L_{aqs} i_q \tag{3.23}$$

The air-gap torque is

$$\begin{aligned} T_e &= \psi_d i_q - \psi_q i_d \\ &= \psi_{ad} i_q - \psi_{aq} i_d \end{aligned} \tag{3.24}$$

With $p\psi_{fd}$ terms and speed variation neglected the stator voltage equations are:

$$\begin{aligned} e_d &= -R_a i_d - \psi_q \\ &= -R_a i_d - \left(L_{l;} i_q - \psi_{aq} \right) \end{aligned} \tag{3.25}$$

$$\begin{aligned} e_q &= -R_a i_q - \psi_d \\ &= -R_a i_q - \left(L_{l;} i_d - \psi_{ad} \right) \end{aligned} \tag{3.26}$$

Machine terminal and infinite bus voltage expressed in term of d-axis and q-axis components is given as follows:

$$\begin{aligned} \widetilde{E}_t &= e_d + j e_q \\ \widetilde{E}_B &= E_{Bd} + j E_{Bq} \end{aligned} \tag{3.27}$$

The network constraint equation for the system shown in figure 3.3 is

$$\begin{aligned}\widetilde{E}_t &= \widetilde{E}_B + (R_E + jX_E)\widetilde{I}_t \\ (e_d + je_q) &= (E_{Bd} + jE_{Bq}) + (R_E + jX_E)(i_d + ji_q)\end{aligned} \tag{3.28}$$

Resolving into d and q components give

$$\begin{aligned}e_d &= R_E i_d - X_E i_q + E_{Bd} \\ e_q &= R_E i_q - X_E i_d + E_{Bq}\end{aligned} \tag{3.29}$$

Where

$$\begin{aligned}E_{Bd} &= E_B \sin\delta \\ E_{Bq} &= E_B \cos\delta\end{aligned} \tag{3.30}$$

Using equations 3.25 and 3.26 to eliminate e_d, e_q in equation 3.29 and using expression for ψ_{aq} and ψ_{ad} given by equation 3.29 we obtain the expression for i_d and i_q as follows:

$$\begin{aligned}i_d &= \frac{X_{Tq}\left[\psi_{fd}\left(\frac{L_{ads}}{L_{ads}+L_{fd}}\right) - E_B\cos\delta\right] - R_T E_B \sin\delta}{D} \\ i_q &= \frac{R_T\left[\psi_{fd}\left(\frac{L_{ads}}{L_{ads}+L_{fd}}\right) - E_B\cos\delta\right] + X_{Td} E_B \sin\delta}{D}\end{aligned} \tag{3.31}$$

Where

$$\begin{aligned}R_T &= R_a + R_E \\ X_{Tq} &= X_E + (L_{aqs} + L_l) = X_E + X_{qs} \\ X_{Td} &= X_E + (L'_{ads} + L_l) = X_E + X'_{ds} \\ D &= R_T{}^2 + X_{Tq}X_{Td}\end{aligned} \tag{3.32}$$

Equation 3.31 together with equations 3.22 and 3.23 can be used to eliminate i_{fd} and T_e from the differential equation 3.15, 3.16 and 3.17 and express them in state variable form. These equations are nonlinear and linearized as shown below:

Expressing equation 3.31 in linearized form yields:

$$\Delta i_d = m_1 \Delta\delta + m_2 \Delta\psi_{fd} \tag{3.33}$$

$$\Delta i_q = n_1 \Delta\delta + n_2 \Delta\psi_{fd} \tag{3.34}$$

Where

$$m1 = \frac{E_B\left(X_{Tq}\sin\delta_o - R_T\cos\delta_o\right)}{D}$$

$$n1 = \frac{E_B\left(R_T\sin\delta_o - X_{Td}\cos\delta_o\right)}{D}$$

$$m_2 = \frac{X_{Tq}}{D}\frac{L_{ads}}{\left(L_{ads}+L_{fd}\right)} \tag{3.35}$$

$$n_2 = \frac{R_T}{D}\frac{L_{ads}}{\left(L_{ads}+L_{fd}\right)}$$

By linearising equation 3.22 and 3.23 and substituting in them the above expressions we get:

$$\Delta\psi_{ad} = L'_{ads}\left(-\Delta i_d + \frac{\Delta\psi_{fd}}{L_{fd}}\right) \tag{3.36}$$

$$= \left(\frac{1}{L_{fd}} - m_2\right)L'_{ads}\Delta\psi_{fd} - m_1 L'_{ads}\Delta\delta$$

$$\Delta\psi_{aq} = -L_{aqs}\Delta i_q \tag{3.37}$$

$$= -n_2 L_{aqs} \Delta\psi_{fd} - n_1 L_{aqs} \Delta\delta$$

Linearizing equation 3.21 and substituting for $\Delta\psi_{ad}$ from equation 3.36 gives

$$\Delta i_{fd} = \frac{\Delta\psi_{fd} - \Delta\psi_{ad}}{L_{fd}}$$

$$= \frac{1}{L_{fd}}\left(1 - \frac{L'_{ads}}{L_{fd}} + m_2 L'_{ads}\right)\Delta\psi_{fd} + \frac{1}{L_{fd}} m_1 L'_{ads} \Delta\delta \qquad (3.38)$$

The linearized form of equation is

$$\Delta T_e = \psi_{ado} \Delta i_q + i_{qo} \Delta\psi_{ad} - \psi_{aqo} \Delta i_d - i_{do} \Delta\psi_{aq} \qquad (3.39)$$

Substituting Δi_q, Δi_d, $\Delta\psi_{ad}$ and $\Delta\psi_{aq}$ from equations 3.33 to 3.37 we obtain

$$\Delta T_e = K_1 \Delta\delta + K_2 \Delta\psi_{fd} \qquad (3.40)$$

Where

$$K_1 = n_1\left(\psi_{ado} + L_{aqs} i_{do}\right) - m_1\left(\psi_{aqo} + L'_{aqs} i_{qo}\right)$$

$$K_2 = n_2\left(\psi_{ado} + L_{aqs} i_{do}\right) - m_2\left(\psi_{aqo} + L'_{aqs} i_{qo}\right) + \frac{L'_{aqs}}{L_{fd}} i_{qo}$$

By linearizng equations 3.15 to 3.17 and substituting the expressions for Δi_{fd} and ΔT_e given by equations 3.38 and 3.40 we obtain the system equations in the desired final form:

$$\begin{bmatrix} \Delta\dot{\omega} \\ \Delta\dot{\delta} \\ \Delta\dot{\psi}_{fd} \end{bmatrix} = \begin{bmatrix} a_{11} & a_{12} & a_{13} \\ a_{21} & 0 & 0 \\ 0 & a_{32} & a_{33} \end{bmatrix} \begin{bmatrix} \Delta\omega \\ \Delta\delta \\ \Delta\psi_{fd} \end{bmatrix} + \begin{bmatrix} b_{11} & 0 \\ 0 & 0 \\ 0 & b_{32} \end{bmatrix} \begin{bmatrix} \Delta T_m \\ \Delta E_{fd} \end{bmatrix} \quad (3.41)$$

Where

$$a_{11} = -\frac{K_D}{2H}$$

$$a_{12} = -\frac{K_1}{2H}$$

$$a_{13} = -\frac{K_2}{2H}$$

$$a_{21} = \omega_o = 2\pi f_o$$

$$a_{32} = -\frac{\omega_o R_{fd}}{L_{fd}} m_1 L'_{ads} \quad (3.42)$$

$$a_{33} = -\frac{\omega_o R_{fd}}{L_{fd}} \left[1 - \frac{L'_{ads}}{L_{fd}} + m_2 L'_{ads} \right]$$

$$b_{11} = \frac{1}{2H}$$

$$b_{32} = \frac{\omega_o R_{fd}}{L_{adu}}$$

And ΔT_m and ΔE_{fd} depends on prime-mover and excitation controls. With constant mechanical input torque, ΔT_m =0; with constant exciter output voltage, ΔE_{fd} =0.

The mutual inductance L_{ads} and L_{aqs} in the above equations are saturated values. The method of accounting for saturation for small signal analysis is described below.

3.3 REPRESENTATION OF SATURATION IN STABILITY STUDIES

In the representation of magnetic saturation for stability studies, the following assumptions are usually made:

a) The leakage inductances are independent of saturation. The leakages fluxes are in air for a considerable portion of their paths so that they are not significantly affected by saturation of the iron portion. As a result, the only elements that saturate are the mutual inductances L_{ad} and L_{aq} .

b) The leakage fluxes do not contribute to the iron saturation. The leakage fluxes are usually small and their paths coincide with that of the main flux for only a small part of its path. By this assumption, saturation is determined by the air-gap flux linkage.

(c) The saturation relationship between the resultant air-gap flux and the mmf under loaded conditions is the same as under no-load conditions. This allows the - saturation characteristics to be represented by the open-circuit saturation curve, which is usually the only saturation data readily available.

(d) There is no magnetic coupling between the d- and q-axes as a result of nonlinearities introduced by saturation; i.e., currents in the windings of one axis do not produce flux that link with the windings of the other axis.

With the above assumptions, the effects of saturation may be represented as

$$L_{ad} = K_{sd} L_{adu}$$

$$L_{aq} = K_{sq} L_{aqu}$$

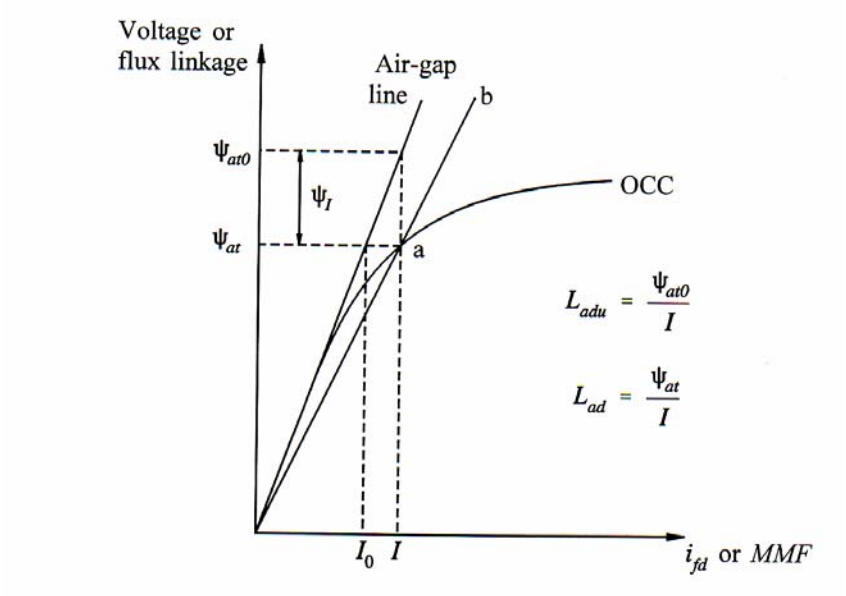

Figure 3.6: Open-circuit characteristics showing effects of saturation.

Where L_{adu} and L_{aqu} are the unsaturated values of L_{ad} and $L_{aq.}$ The saturation factor Ksd and Ksq identifies the degrees of saturation in the d-axis and q-axis respectively.

The saturation curve may be divided into three segments:

I. Unsaturated segment

II. Nonlinear segment

III. Fully saturated linear segment.

The threshold values ψ_{T1} and ψ_{T2} defines the boundaries of the three segments as shown in figure 3.7.

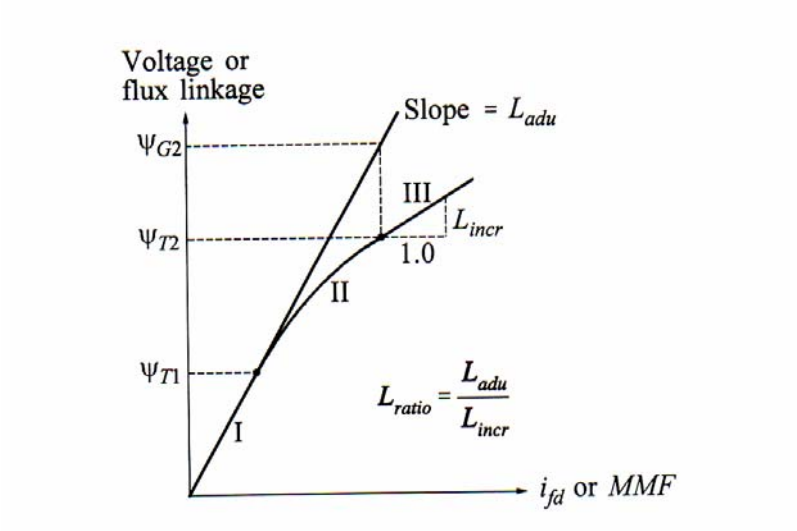

Figure 3.7: Representation of saturation characteristics.

Since we are expressing small-signal performance in terms of perturbation values of flux linkage and currents, a distinction has to be made between total saturation and incremental saturation.

Total saturation is associated with total values of flux linkages and currents. Incremental saturation is associated with perturbed values of flux linkages and currents. Therefore the incremental slope of the saturation curve is used in computing the incremental saturation as shown in Figure 3.10.

Denoting the incremental saturation factor $K_{sd(incr)}$ we have:

$$L_{ads(incr)} = K_{sd(incr)} L_{adu} \tag{3.43}$$

Also we can show that

$$K_{sd(incr)} = \frac{1}{1 + B_{sat} A_{sat} e^{B_{sat}(\psi_{ato} - \psi_{T1})}} \tag{3.44}$$

Where A_{sat} and B_{sat} are saturation constants depending on the saturation characteristics in the segment II portion in figure 3.8.

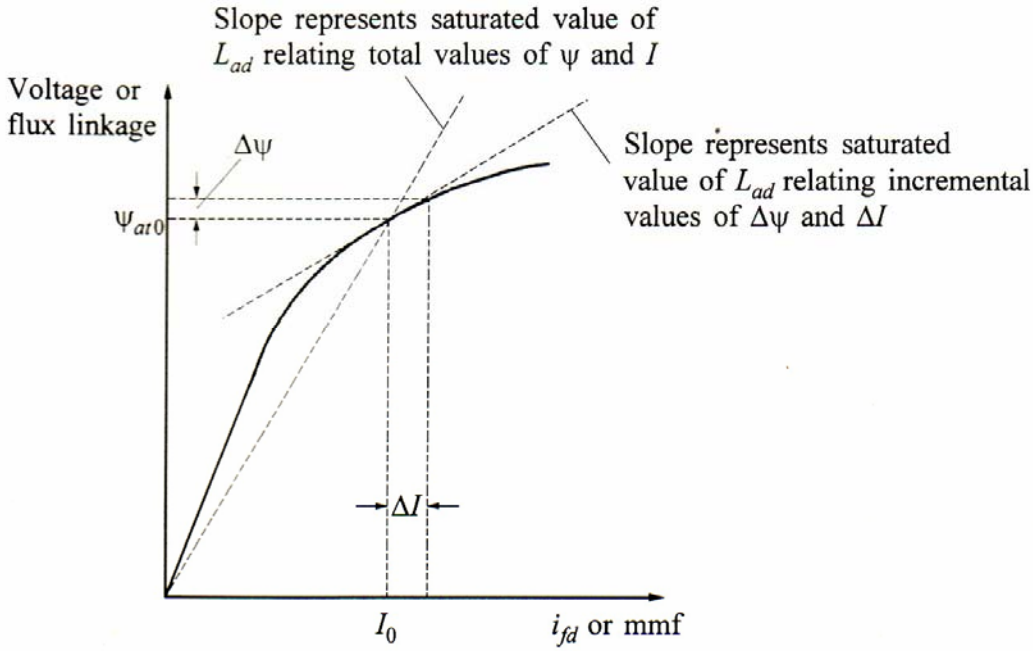

Figure 3.8: Distinction between incremental and total saturation

For computing the initial values of system variable (denoted by subscript o), total saturation is used. For relating the perturbed values, i.e., in equation 3.32, 3.35, 3.40 and 3.42 the incremental saturation factor is used.

Figure 3.9 shows the block diagram representation of the small signal performance of the system.

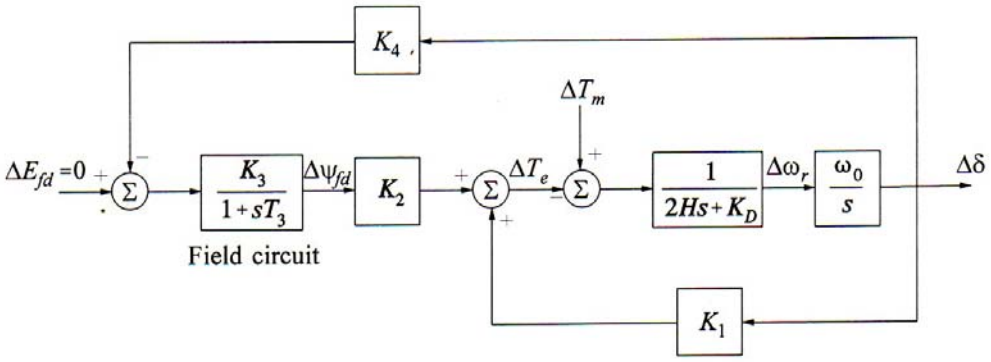

Figure 3.9 Block Diagram representation with constant E_{fd}

In this representation, the dynamic characteristics of the system are expressed in terms of the K-constants.

From equation 3.40, we may express the change in air-gap torque as a function of $\Delta\delta$ and $\Delta\psi_{fd}$ as follows:

$$\Delta T_e = K_1\Delta\delta + K_2\Delta\psi_{fd}$$

Where:

$$K_1 = \frac{\Delta T_e}{\Delta\delta} \quad \text{With constant } \Delta\psi_{fd}$$

$$K_2 = \frac{\Delta T_e}{\Delta\psi_{fd}} \quad \text{With constant rotor angle } \Delta\delta$$

The component of torque given by $K_1\Delta\delta$ is in phase with $\Delta\delta$ and hence represents a synchronizing torque component.

The component of torque resulting from variations in field flux linkage is given by $K_2\Delta\psi_{fd}$.

The variation of $\Delta\psi_{fd}$ is determined by the field circuit dynamic equation:

$$p\Delta\psi_{fd} = a_{32}\Delta\delta + a_{33}\Delta\psi_{fd} + b_{32}\Delta E_{fd} \tag{3.45}$$

By grouping terms involving $\Delta\psi_{fd}$ and rearranging, we get

$$\Delta\psi_{fd} = \frac{K_3}{1+pT_3}\left[\Delta E_{fd} - K_4\Delta\delta\right] \tag{3.46}$$

Where:

$$K_3 = -\frac{b_{32}}{a_{33}}$$

$$K_4 = -\frac{a_{32}}{b_{32}} \tag{3.47}$$

$$T_3 = -\frac{1}{a_{33}} = K_3 T'_{do}\frac{L_{adu}}{L_{ffd}}$$

3.4 EFFECT OF FIELD FLUX VARIATION ON SYSTEM STABILITY

The change in air-gap torque due to field flux variations caused by rotor angle changes is given by

$$\left.\frac{\Delta T_e}{\Delta\delta}\right|_{due.to.\Delta\psi_{fd}} = -\frac{K_1K_2K_4}{1+sT_3} \tag{3.48}$$

The constants K_2, K_3 and K_4 are usually positive. The contribution of $\Delta\psi_{fd}$ to synchronizing and damping torque components depends on the oscillatory frequency as shown below:

(a) In the steady state and at very low frequencies ($s = j\omega \rightarrow 0$):

ΔT_e due to $\Delta\psi_{fd} = -K_2K_3K_4\Delta\delta$

The field flux variation due to $\Delta\delta$ feedback introduces a negative synchronizing torque component. The system becomes monotonically unstable when this exceeds $K_1 \Delta\delta$. The steady-state stability limit is reached when

$$K_2K_3K_4 = K_1$$

(b) At oscillatory frequencies much higher than $1/T_3$:

$$\Delta T_3 \approx -\frac{K_2 K_3 K_4}{j\omega T_3}\Delta\delta$$

$$= \frac{K_2 K_3 K_4}{\omega T_3} j\Delta\delta$$

Thus, the component of air-gap torque due to $\Delta\psi_{fd}$ is 90^o ahead of $\Delta\delta$ or in phase with $\Delta\omega$. Hence, $\Delta\psi_{fd}$ results in a positive damping torque component.

(c) At typical machine oscillating frequencies of about 1Hz, $\Delta\psi_{fd}$ results in a positive damping torque component and a negative synchronizing torque component. The net effect is to reduce slightly the synchronizing torque component and increase the damping torque component.

Special situation with K_4 negative:

The coefficient K_4 is normally positive. As long as it is positive, the effect of field flux variation due to armature reaction is to introduce a positive damping torque component. However, there can be situation where K_4 is negative. K_4 is negative when a hydraulic generator without damper windings is operating at light load and is connected by a line of relatively high resistance to reactance ratio to a large system.

Also K_4 can be negative when a machine is connected to a large local load, supplied partly by the generator and partly by the remote large system. Under such conditions, the

torques produced by induced currents in the field due to armature reaction has components out of phase with $\Delta\omega$, and produce negative damping.

CHAPTER 4

EFFECT OF EXCITATION SYSTEM

Under effect of excitation system state-space model and the block diagram developed in the previous section is extended to include the excitation system. Then the effect of the excitation system on the small-signal stability performance of the single-machine infinite bus system is considered.

The input control signal to the excitation system is normally the generator terminal voltage E_t. $\widetilde{E}_t$ May be expressed in complex form:

$$\widetilde{E}_t = e_d + je_q$$

Hence,

$$E_t^{\,2} = e_d^{\,2} + e_q^{\,2}$$

Appling a small perturbation, we may write

$$\left(E_{to} + \Delta E_t\right)^2 = (e_{d0} + \Delta e_d)^2 + (e_{q0} + \Delta e_q)^2$$

By neglecting higher order terms in above expression, the above equation reduced to

$$E_{to}\Delta E_t = e_{d0}\Delta e_d + e_{q0}\Delta e_q$$

Therefore,

$$\Delta E_t = \frac{e_{d0}}{E_{to}}\Delta e_d + \frac{e_{q0}}{E_{to}}\Delta e_q \qquad (4.1)$$

In terms of the perturbed values, equations 3.25 and 3.26 may be written as:

$$\Delta e_d = -R_a\Delta i_d - \left(L_l\Delta i_q - \Delta\psi_{aq}\right) \qquad (4.2)$$

$$\Delta e_q = -R_a\Delta i_q - \left(L_l\Delta i_d - \Delta\psi_{ad}\right) \qquad (4.3)$$

Using equations 3.33, 3.34, 3.36 and 3.37 to eliminate Δi_d , Δi_q , $\Delta\psi_{ad}$ and $\Delta\psi_{aq}$ from the above equations in terms of the state variables and substituting the values form equations form 4.2 and 4.3 in 4.1 we get:

$$\Delta E_t = K_5\Delta\delta + K_6\Delta\psi_{fd} \qquad (4.4)$$

Where (4.5)

$$K_5 = \frac{e_{d0}}{E_{to}}[-R_a m_1 + L_l n_1 + L_{aqs} n_1] + \frac{e_{q0}}{E_{to}}[-R_a n_1 + L_l m_1 + L'_{ads} m_1]$$

$$K_6 = \frac{e_{d0}}{E_{to}}[-R_a m_2 + L_l n_2 + L_{aqs} n_2] + \frac{e_{q0}}{E_{to}}\left[-R_a n_2 + L_l m_2 + L'_{ads}\left(\frac{1}{L_{fd}} - m_2\right)\right]$$

The influence on small-signal stability is examined by considering the excitation system model shown in Figure 4.1. It is representative of thyristor excitation systems. The model shown in Figure 4.1, however, has been simplified to include only those elements that are considered necessary for representing a specific system. A high exciter gain, without transient gain reduction or derivative feedback, is used. Parameter TR represents the terminal voltage transducer time constant.

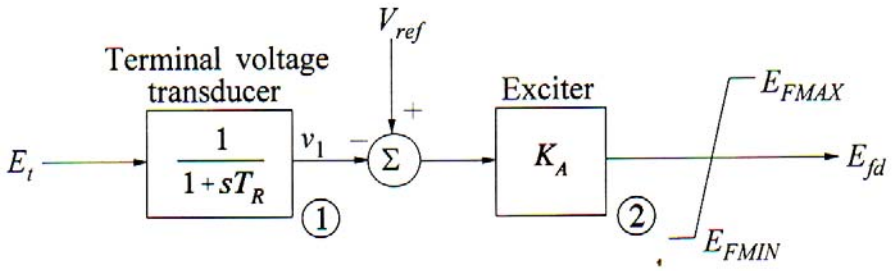

Figure 4.1 Thyristor excitation system with AVR

The only nonlinearity associated with the model is that due to the ceiling on the exciter output voltage represented by E_{FMAX} and E_{FMIN}. For small-disturbance studies, these limits are ignored as we are interested in a linearized model about an operating point such that E_{fd} is within the limits. Limiters and protective circuits are not modeled as they do not affect small-signal stability.

From block of figure 4.1, using perturbed values, we have

$$\Delta v_1 = \frac{1}{1 + pT_R}\Delta E_t$$

Hence,

$$p\Delta v_1 = \frac{1}{T_R}(\Delta E_t - \Delta v_1)$$

Substituting for ΔE_t from 4.4 we get:

$$p\Delta v_1 = \frac{1}{T_R}(K_5\Delta\delta + K_6\Delta\psi_{fd} - \Delta v_1) \tag{4.6}$$

From block 2 of figure 4.1 we get

$$E_{fd} = K_A(V_{ref} - v_1)$$

In terms of perturbed values we have

$$\Delta E_{fd} = K_A(-\Delta v_1) \tag{4.7}$$

The field circuit dynamic equation shown in equation 3.45 becomes:

$$p\Delta\psi_{fd} = a_{31}\Delta\omega_r + a_{32}\Delta\delta + a_{33}\Delta\psi_{fd} + a_{34}\Delta v_1 \tag{4.8}$$

Where,

$$a_{34} = -b_{32}K_A = -\frac{\omega_o R_{fd}}{L_{adu}}K_A \tag{4.9}$$

The expressions for a_{31}, a_{32} and a_{33} remain unchanged as before and since we have a first order-order model for the exciter, the order of the overall system is increased by 1; the new state variable added is Δv_1:

$$\Delta v_1 = a_{41}\Delta\omega_r + a_{42}\Delta\delta + a_{43}\Delta\psi_{fd} + a_{44}\Delta v_1 \tag{4.10}$$

Where,

$$
\begin{aligned}
a_{41} &= 0 \\
a_{42} &= \frac{K_5}{T_R} \\
a_{43} &= \frac{K_6}{T_R} \\
a_{44} &= -\frac{1}{T_R}
\end{aligned}
\tag{4.11}
$$

The complete state-space model for the power system, including the excitation system of figure 4.1 has the following form:

$$
\begin{bmatrix} \Delta\dot{\omega}_r \\ \Delta\dot{\delta} \\ \Delta\dot{\psi}_{fd} \\ \Delta\dot{v}_1 \end{bmatrix} = \begin{bmatrix} a_{11} & a_{12} & a_{13} & 0 \\ a_{21} & 0 & 0 & 0 \\ 0 & a_{32} & a_{33} & a_{34} \\ 0 & a_{42} & a_{43} & a_{44} \end{bmatrix} \begin{bmatrix} \Delta\omega_r \\ \Delta\delta \\ \Delta\psi_{fd} \\ \Delta v_1 \end{bmatrix} + \begin{bmatrix} b_1 \\ 0 \\ 0 \\ 0 \end{bmatrix} \Delta T_m \tag{4.12}
$$

For constant mechanical torque input

$$\Delta T_m = 0$$

4.1 BLOCK DIAGRAM REPRESENTATION

Figure 4.2 shows the block diagram obtained by extending figure 3.11 to include the voltage transducer and Automatic Voltage Regulator/ Exciter block. The representation is applicable to any type of exciter, with $G_{ex}(s)$ representing the transfer function of the AVR and exciter. For a thyristor exciter,

$$G_{ex}(s) = K_A$$

The terminal voltage error signal, which forms the input to the voltage transducer block, is given by Equation 4.4:

$$\Delta E_t = K_5 \Delta\delta + K_6 \Delta\psi_{fd}$$

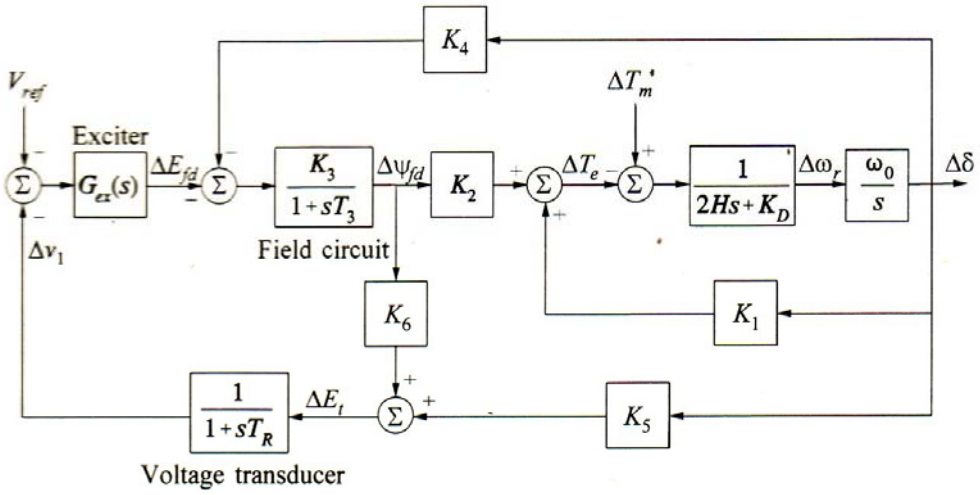

Figure 4.2 Block diagram representation with exciter and AVR

The coefficient K_6 is always positive, whereas K_5 can be either positive or negative, depending on the operating condition and the external network impedance R_E+jX_E. The value of K_5 has a significant bearing on the influence of the AVR on the damping of system oscillations.

4.2 EFFECT OF AVR ON SYNCHRONIZING AND DAMPING TORQUE COMPONENT

We were normally interested in the performances of excitation systems with moderate or high responses. For such excitation systems, we can make the following general observations regarding the effects of the AVR:

- With K_5 positive, the effect of the AVR is to introduce a negative synchronizing torque and a positive damping torque component.

  The constant K_5 is positive for low values of external system reactance and low generator outputs.

  The reduction in K_S due to AVR action in such cases is usually of no particular concern, because K_1 is so high that the net K_S is significantly greater than zero. Component and a negative damping torque component. This effect is more pronounced as the exciter response increases

- With K_5 negative, the AVR action introduces a positive synchronizing torque.

  For high values of external system reactance and high generator outputs K_5 is negative. In practice, the situation where K_5 is negative are commonly encountered. For such cases, a high response exciter is beneficial in increasing synchronizing torque. However, in so doing it introduces negative damping. We thus have conflicting requirements with regard to exciter response. One possible recourse is to strike a compromise and set the exciter response so that it results in sufficient synchronizing and damping torque components for the expected range of system-operating conditions. This may not always be possible. It may be necessary to use a high-response exciter to provide the required synchronizing torque and transient stability performance. With a very high external system reactance, even with low exciter response the net damping torque coefficient may be negative.

.

4.3 OBSERVATIONS WITH AVR ONLY

Model used in Simulink to simulate the effect of excitation and AVR on the single machine infinite bus system is shown in figure 4.3.

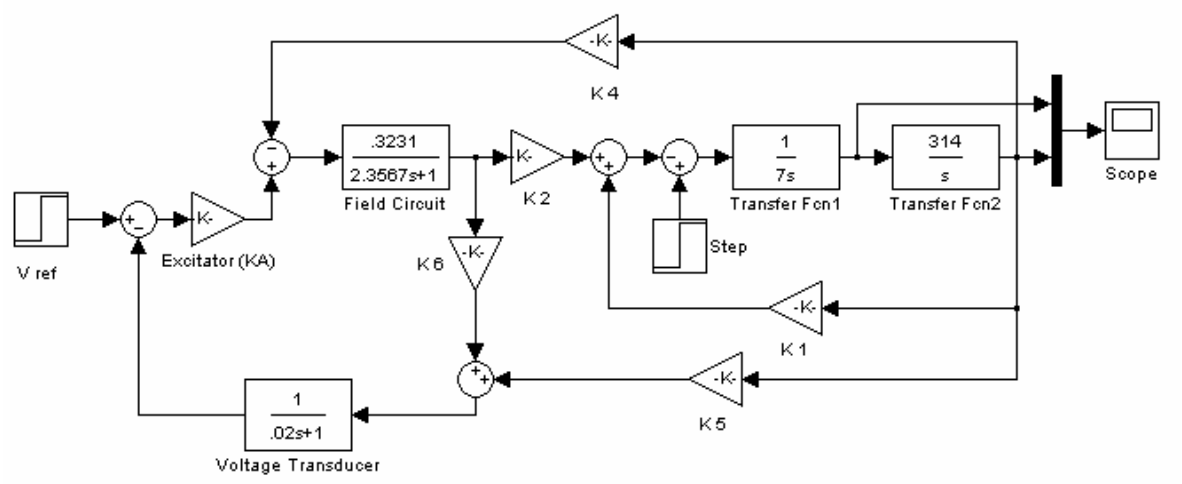

Figure 4.3: Simulink model for simulation of infinite bus system with AVR only

Parameter consideration for the above model:

System operating condition in per unit for 4×555 MVA, 24 KV, 50 Hz generating unit on a common 2220MVA, 24 KV base are:

P=0.9; Q=P/3; E_t=1.0

Thyristor exciter gain:

K_A=200; T_R=0.02;

Frequency of oscillation is taken as 10 rad/sec

Values of other parameters

f=50;	Xd=1.81;	Xq=1.76;	Xd1=0.3;
XL=0.16;	Xe=0.65;	Ra=0.003;	Tdo1=8.0;
H=3.5;	K_A=200;	ωo=314;	
W=10;	K_D=0;	T_R=0.02;	

Values of 'K' constants calculated using above parameters:

K1 =0.7636

K2 =0.8644

K3 =0.3231

K4 = 1.4189

K5 = -0.1463

K6 =0.4167

Change in the time response of the system for the 5% change in mechanical input is figure 4.3, depicts that the system is unstable.

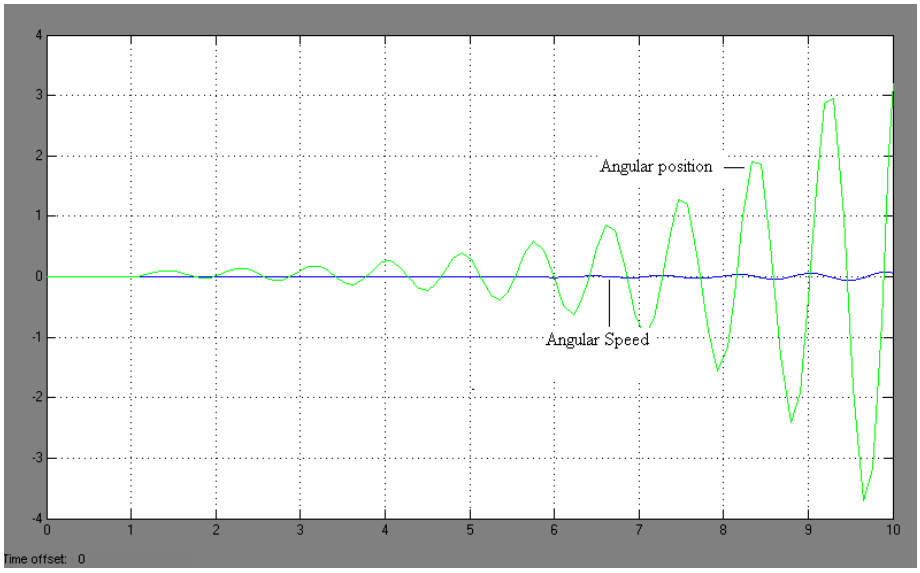

Figure 4.4 System Response for 5% change in ΔT_m

4.4 PROBLEM IDENTIFICATION

With AVR, constant K_5 may have either negative of positive values as shown in figure 4.5, which in influence the damping and synchronizing torque coefficient.

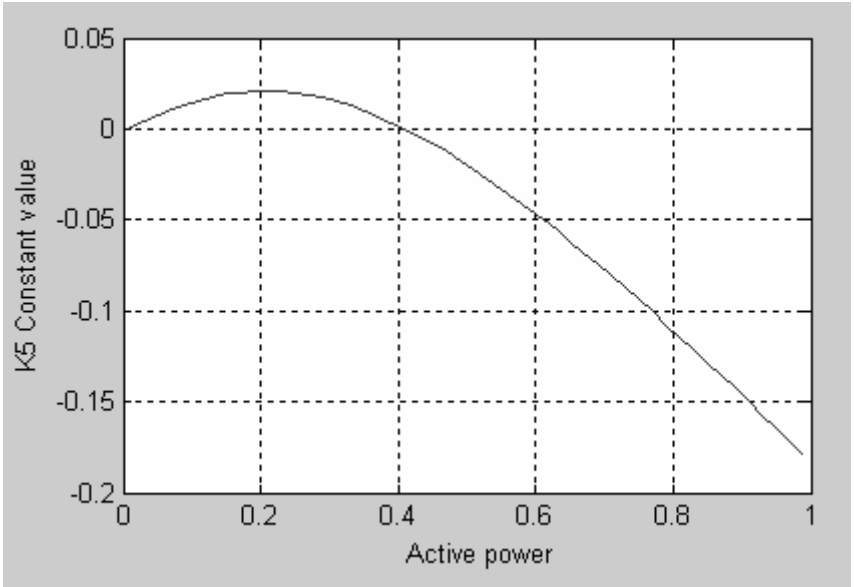

Figure 4.5 Variation of K_5 with per unit active power

The effect of AVR is to introduce positive synchronizing coefficient and negative damping coefficient which is as evident in figure 4.6 and 4.7

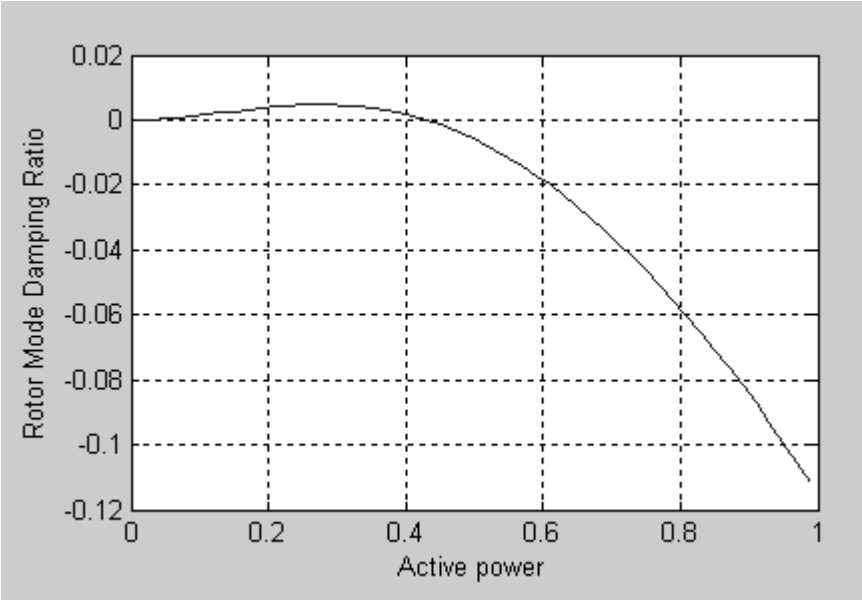

Figure 4.6 Variation of Damping Torque Coefficient with per unit power

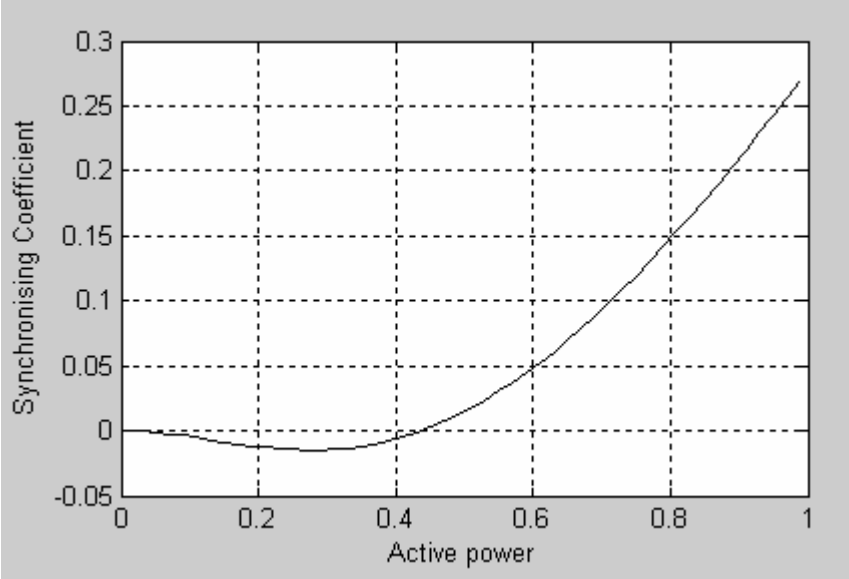

Figure 4.7 Variation of Synchronizing Coefficient with per unit power

Now effect **variation in excitation** on system stability will be portrayed. Value of excitation to the system is controlled by excitation gain K_A. So K_A will be varied its effect on the damping torque coefficient and synchronizing coefficient will be studied. K_5 is independent of K_A so its effect will not be taken into account.

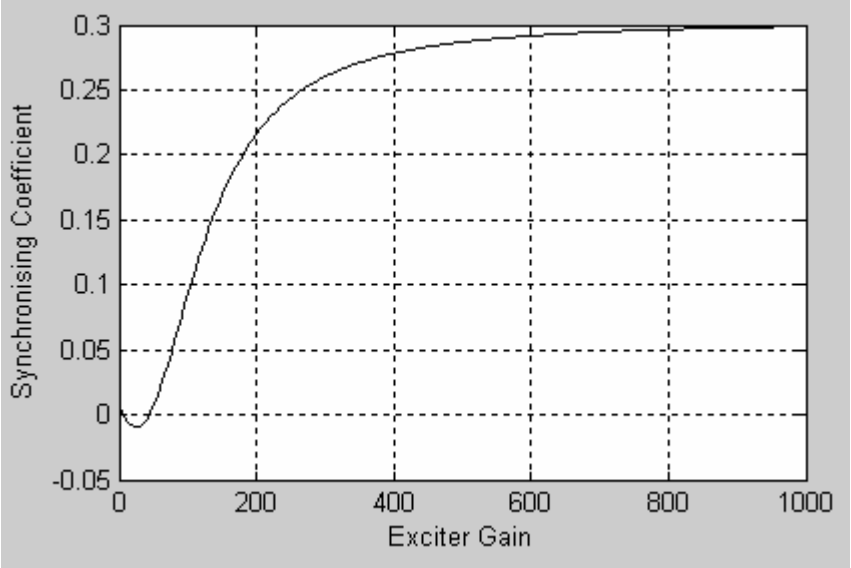

Figure 4.8 Variation of Synchronizing coefficient K_S With K_A

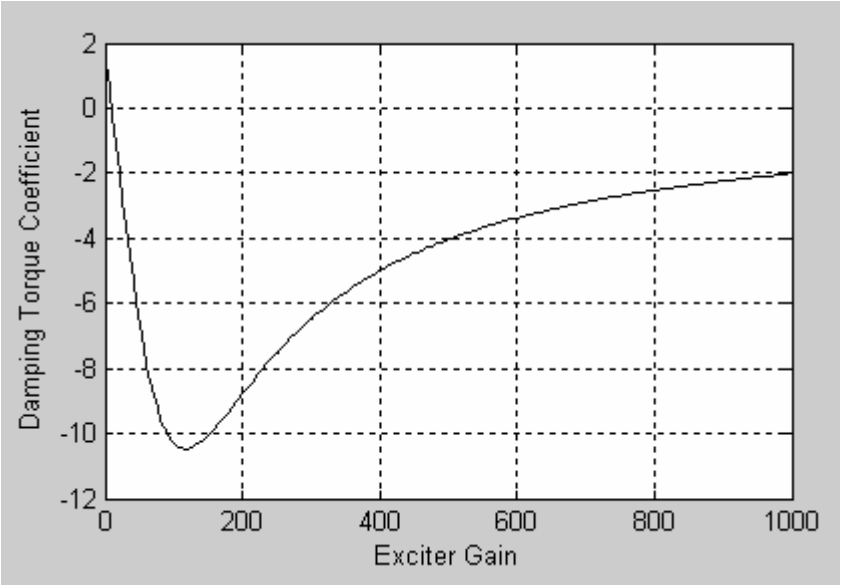

Figure 4.9 Variation of damping torque coefficient with K_A

The effect of the variation in exciter gain (K_A) on synchronizing and damping coefficient is shown in figure 4.8 and 4.9. Where, for lower excitation the damping torque coefficient is more negative. The net damping is smallest when K_A is 110(approx.) and will increase with increase in exciter gain. But there is certain limit utpo which exciter gain can be increased. The high response exciter is beneficial in increasing synchronizing torque but in doing so it introduces negative damping this is as evident in figure 4.8 and 4.9.

From the above analysis, we concluded that the effect of AVR on damping and synchronizing torque component is thus primarily influence by constant K_5 and exciter gain K_A. With constant K_5 negative, the AVR action introduces a positive synchronizing torque component and negative damping torque component. This effect is more pronounced as this exciter response increases. The main cause of instability of the system is negative damping coefficient; this adverse affect of low damping should be removed by adding damping to the system. So these under damped oscillations in power system call for the new approach i.e. power system stabilizer and later fuzzy logic based power system stabilizer.

CHAPTER 5

POWER SYSTEM STABILIZER

The basic function of a power system stabilizer (PSS) is to add damping to the generator rotor oscillations by controlling its excitation using auxiliary stabilizing signal(s). To provide damping, the stabilizer must produce a component of electrical torque in phase with the rotor speed deviations.

The theoretical basis for a PSS may be illustrated with the aid of the block diagram shown in Figure 5.1. This is an extension of the block diagram of Figure 4.2 and includes the effect of a PSS.

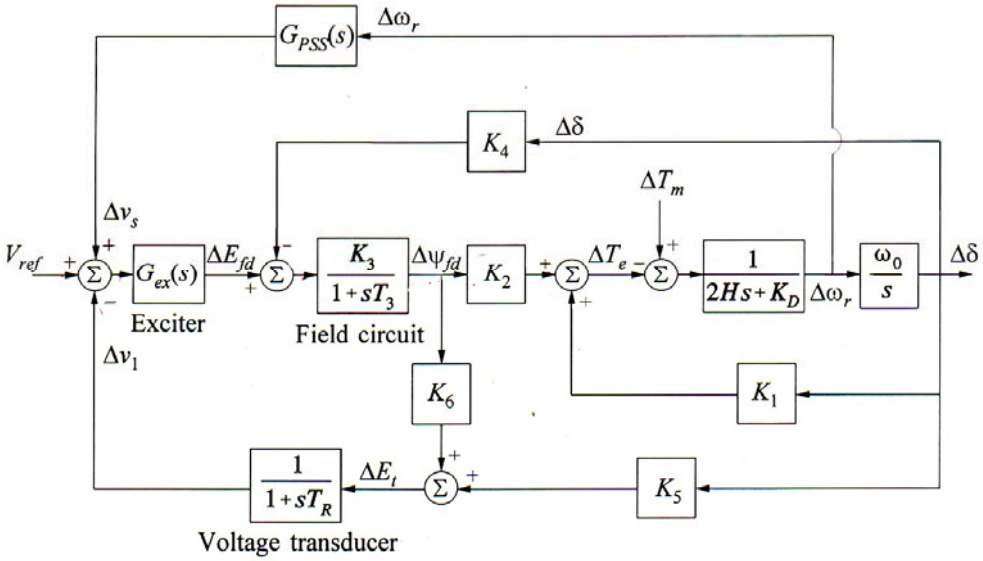

Figure 5.1 Block diagram representation with AVR and PSS

Since the purpose of a PSS is to introduce a damping torque component. A logical signal to use for controlling generator excitation is the speed deviation $\Delta\omega_r$.

If the exciter transfer function $G_{ex}(s)$ and the generator transfer function between ΔE_{fd} and ΔT_e, were pure gains, a direct feedback of $\Delta\omega_r$, would result in a damping torque component. However, in practice both the generator and the exciter (depending on its type) exhibit frequency dependent gain and phase characteristics. Therefore, the PSS transfer function, $G_{PSS}(s)$, should have appropriate phase compensation circuits to compensate for the phase lag between the exciter input and the electrical torque. In the ideal case, with the phase characteristic of $G_{PSS}(s)$ being an exact inverse of the exciter and generator phase characteristics to be compensated, the PSS would result in a pure damping torque at all oscillating frequencies.

Structure, modelling, and performance of power system stabilizers will now be illustrated by considering a thyristor excitation system. Figure 5.2 shows the block diagram of the excitation system, including the, AVR and PSS. Since we are concerned with small-

signal performance, stabilizer output limits and exciter output limits are not shown in the figure. The following is a brief description of the basis for the PSS configuration and considerations in the selection of the parameters.

5.1 PSS COMPOSITION

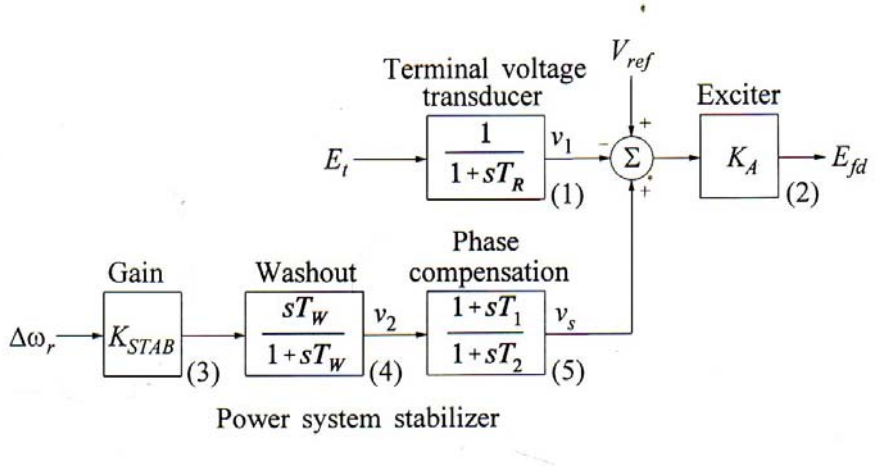

Figure 5.2 Thyristor excitation system with AVR and PSS

The **phase compensation** block provides the appropriate phase-lead characteristic to compensate for the phase lag between the exciter input and the generator electrical (air-gap) torque. The figure shows a single first-order block. In practice two or more first-order blocks may be used to achieve the desired phase compensation. In some cases, second-order blocks with complex roots have been used.

Normally, the frequency range of interest is 0.1 to 3.0 Hz, and the phase-lead network should provide compensation over this entire frequency range. The phase characteristic to be compensated changes with system conditions; therefore, a compromise is made and a characteristic acceptable for different system conditions is selected. Generally some under compensation is desirable so that the PSS, in addition to significantly increasing the damping torque, results in a slight increase of the synchronizing torque.

The **signal washout** block serves as a high-pass filter, with the time constant T_w, high enough to allow signals associated with oscillations in ω_r to pass unchanged, which removes dc signals. Without it, steady changes in speed would modify the terminal voltage. It allows the power system stabilizer to respond only to changes in speed. From the viewpoint of the washout function, the value of T_w is not critical and may be in the range of 1 to 20 seconds. The main consideration is that it is long enough to pass stabilizing signals at the frequencies of interest unchanged, but not so long that it leads to undesirable generator voltage excursions during system-islanding conditions.

The **stabilizer gain** K_{STAB} determines the amount of damping introduced by the PSS. Ideally, the gain should be set at a value corresponding to maximum damping; however, it is often limited by other considerations.

5.2 STATE SPACE REPRESENTATION WITH PSS

From block 4 of Figure 5.2, using perturbed values, we have

$$\Delta v_2 = \frac{pT_W}{1+pT_W}(K_{STAB}\Delta\omega_r)$$

Hence,

$$p\Delta v_2 = K_{STAB}\,p\Delta\omega_r - \frac{1}{T_W}\Delta v_2 \qquad (5.1)$$

Substituting for $p\Delta\omega_r$ given by Equation 3.41, we obtain the following expression for $p\Delta v_2$ in terms of the state variables:

$$p\Delta v_2 = K_{STAB}\left[a_{11}\Delta\omega_r + a_{12}\Delta\delta + a_{13}\Delta\psi_{fd} + \frac{1}{2H}\Delta T_m \right] - \frac{1}{T_W}\Delta v_2$$

$$= a_{51}\Delta\omega_r + a_{52}\Delta\delta + a_{53}\Delta\psi_{fd} + a_{54}\Delta v_2 + \frac{K_{STAB}}{2H}\Delta T_m \quad (5.2)$$

Where,

$$\begin{aligned} a_{51} &= K_{STAB}a_{11} \\ a_{52} &= K_{STAB}a_{12} \\ a_{53} &= K_{STAB}a_{13} \\ a_{55} &= \frac{1}{T_W} \end{aligned} \quad (5.3)$$

From block 5,

$$\Delta v_s = \Delta v_2\left(\frac{1+pT_1}{1+pT_2}\right)$$

Hence

$$p\Delta v_s = \frac{T_1}{T_2}p\Delta v_2 + \frac{1}{T_2}\Delta v_2 - \frac{1}{T_2}\Delta v_s$$

Substitution for $p\Delta v_2$, given by equation 5.2, yields

$$p\Delta v_s = a_{61}\Delta\omega_r + a_{62}\Delta\delta + a_{63}\Delta\psi_{fd} + a_{64}\Delta v_1 + a_{65}\Delta v_2 + a_{66}\Delta v_s + \frac{T_1}{T_2}\frac{K_{STAB}}{2H}\Delta T_m$$

…….....(5.4)

Where,

$$
\begin{aligned}
a_{61} &= \frac{T_1}{T_2} a_{51} \\
a_{62} &= \frac{T_1}{T_2} a_{52} \\
a_{63} &= \frac{T_1}{T_2} a_{53} \\
a_{65} &= \frac{T_1}{T_2} a_{55} + \frac{1}{T_2} \\
a_{63} &= -\frac{1}{T_2}
\end{aligned}
\tag{5.5}
$$

From block 2 we get,

$$\Delta E_{fd} = K_A(\Delta v_s - \Delta v_1)$$

The field circuit equation, with PSS included, becomes

$$p\Delta\psi_{fd} = a_{32}\Delta\delta + a_{33}\Delta\psi_{fd} + a_{34}\Delta v_2 + a_{36}\Delta v_S \tag{5.6}$$

Where,

$$a_{36} = \frac{\omega_o R_{fd}}{L_{adu}} K_A \tag{5.7}$$

The complete state-space model, including the PSS, has the following form (with $\Delta T_m = 0$);

$$\begin{bmatrix} \Delta\dot{\omega}_r \\ \Delta\dot{\delta} \\ \Delta\dot{\psi}_{fd} \\ \Delta\dot{v}_1 \\ \Delta\dot{v}_2 \\ \Delta\dot{v}_S \end{bmatrix} = \begin{bmatrix} a_{11} & a_{12} & a_{13} & 0 & 0 & 0 \\ a_{31} & 0 & 0 & 0 & 0 & 0 \\ 0 & a_{32} & a_{33} & a_{34} & 0 & a_{36} \\ 0 & a_{42} & a_{43} & a_{44} & 0 & 0 \\ a_{51} & a_{52} & a_{53} & 0 & a_{55} & 0 \\ a_{61} & a_{62} & a_{63} & 0 & a_{65} & a_{66} \end{bmatrix} \begin{bmatrix} \Delta\omega_r \\ \Delta\delta \\ \Delta\psi_{fd} \\ \Delta v_1 \\ \Delta v_2 \\ \Delta v_S \end{bmatrix} \qquad (5.8)$$

5.3 SELECTION OF PSS PARAMETERS

The overall excitation control system is designed so as to:

- Maximize the damping of the local plant mode as well as inter-area mode oscillations without compromising the stability of other modes;
- Enhance system transient stability;
- Not adversely affect system performance during major system upsets which cause large frequency excursions; and
- Minimize the consequences of excitation system malfunction due to component failures.

The block diagram of the PSS used to achieve the desired performance objectives is shown in Figure 5.2. Some of the considerations and procedures for the selection of PSS parameters were already discussed under PSS composition. Here check on selected settings will be performed.

The final stage in stabilize design involves the evaluation of its effect on the overall system performance. First, the effect of the stabilizer on various modes of system oscillations is determined over a wide range of system conditions by using a small-signal stability program. This includes analysis of the effects of the PSS on

local plant modes, inter area modes, and control modes. In particular, it is important to ensure that there are no adverse interactions with the controls of other nearby generating units and devices.

The excitation control systems, designed and describe above, provide effective decentralized controllers for the damping of electromechanical oscillations in power systems. Generally, the resulting design is much more robust that can be achieved through use of other methods. The overall approach is used on acknowledgement of the physical aspects of the power system stabilization problem. The method used for establishing the characteristics of the PSS is simple and required only the dynamic characteristics of the concerned machines to be modeled in detail. Detailed analysis of the performance of the power system is used to establish other parameters and to ensure adequacy of the overall performance of the excitation control. The result is a control that enhances the overall stability of the system under different operating conditions. Since the PSS is tuned to increase the damping torque component for wide range of frequencies, it contributes to the damping of all system modes in which the respective generator has a high participation. This includes any new mode that may emerge as a result of changing system conditions. It is possible to satisfy the requirements for a wide range of system conditions with fixed parameters.

Here, the effects of stabilizer on various modes of oscillations are determined for a wide range of system conditions using eigen value programs. Also the effect of stabilizer was determined using discrete domain.

5.4 OBSERVATION WITH PSS AND AVR

Model used in Simulink/ Matlab to examine the effect of power system stabilizer with automatic voltage regulator on single machine infinite bus system is shown below in figure 5.3

.

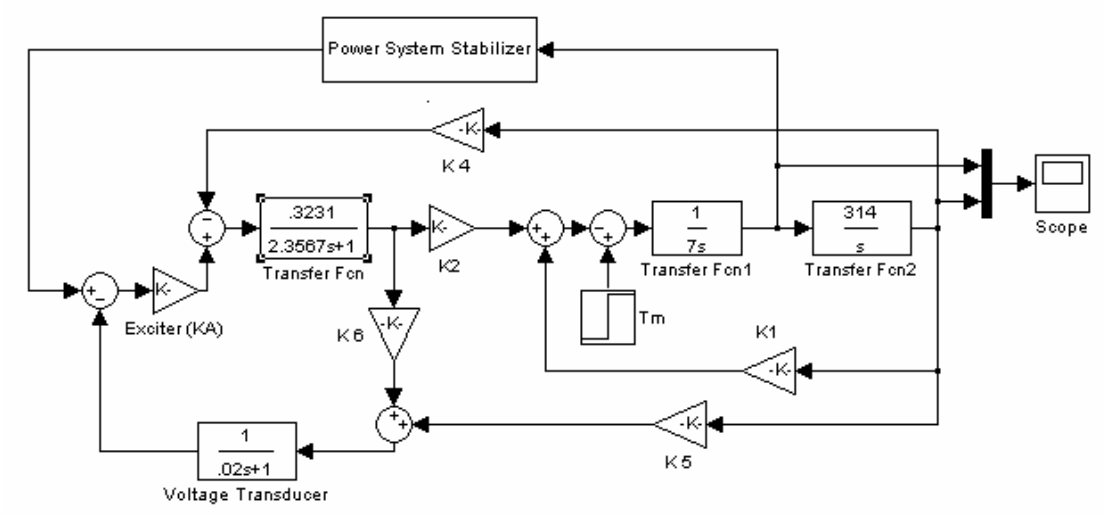

Figure 5.3 Simulink Model with AVR and PSS

Power System Stabilizer subsystem also composed of three blocks: a phase compensation block, a signal washout block, and a gain block. Expanded form of Power System Stabilizer block is shown in figure below:

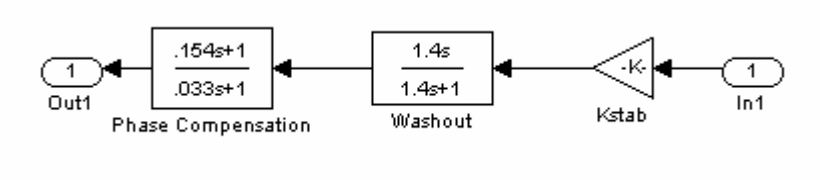

Figure 5.4 Power System Stabilizer block

PARAMETERS CONSIDERATIONS FOR THE SYSTEMS SHOWN IN FIGURE 5.3 AND 5.4

System operating condition in per unit for 4×555 MVA, 24 KV, 50 Hz generating unit on a common 2220MVA, 24 KV base are:

P=0.9; Q=P/3; E_t=1.0

Thyristor exciter gain:

K_A=200; T_R=0.02;

Frequency of oscillation is taken as 10 rad/sec.

Parameters of power system stabilizer: T_1=0.154

T_2=0.033 T_W=1.4 K_{STAB}=9.5;

Values of other parameters

f=50; X_d=1.81; X_q=1.76;

X_{dl}=0.3; X_L=0.16; Xe=0.65; Ra=0.003;

T_{do1}=8.0; H=3.5; K_A=200;

ω_o=314; ω=10; K_D=0;

T_R=0.02; E_T=1.0; E_{Tmag}=1.0; L_{adu}=1.65;

L_{aqu}=1.60; L_L=0.16; R_{fd}=0.0006;

L_{fd}=0.153; K_{sd}=0.8491; K_{sq}=0.8491;

K_{sdl}=0.434; K_{sql}=0.434;

Saturation Constant used:

A_{SAT}=0.031; B_{SAT}=6.93; ψ_1 =0.8;

With above constants we for the model shown in figure 5.3 we will analyze the variation of angular speed and angular position with time this is shown in figure 5.5 and 5.6 in the figure below

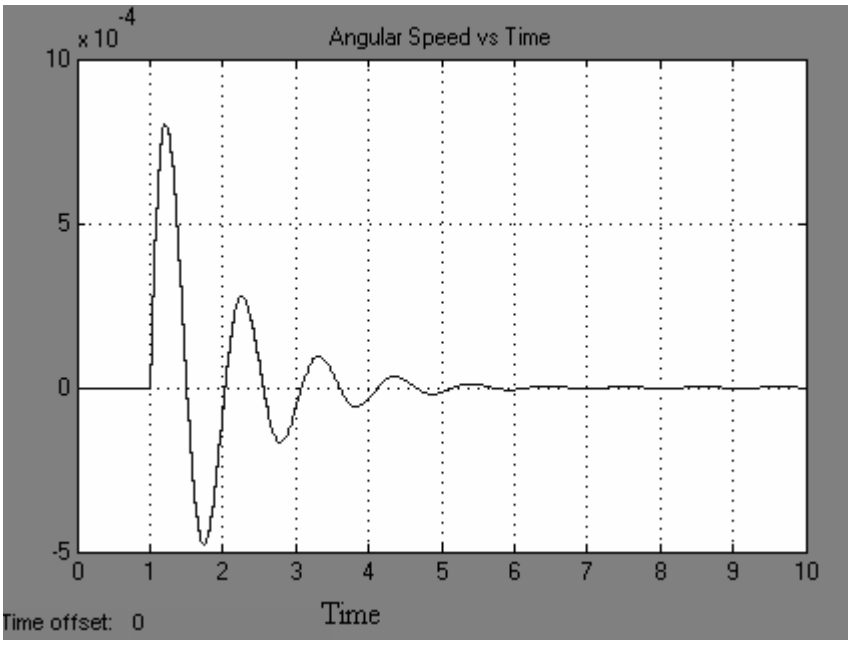

Figure 5.5 Variation of Angular Speed with Time

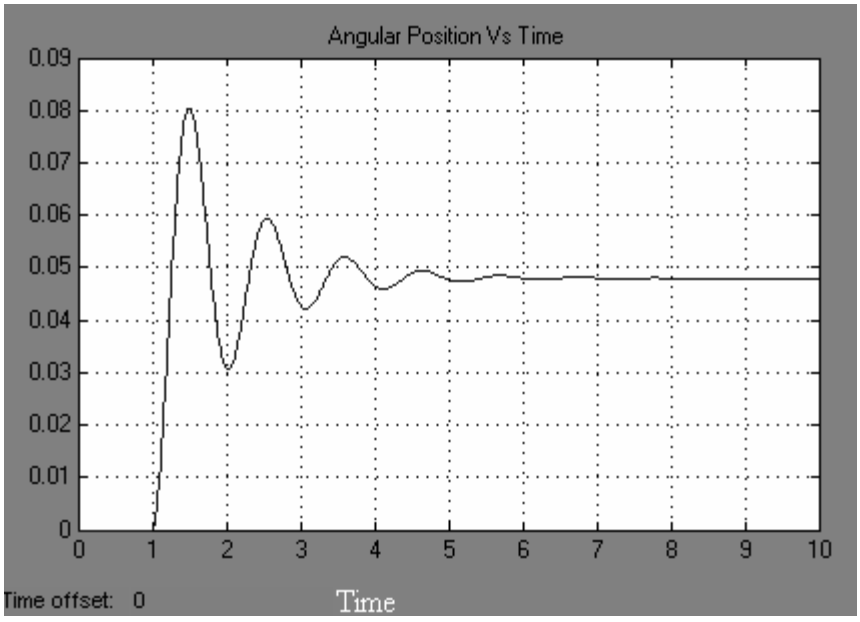

Figure 5.6 Variation of Angular position with Time

Examining the variation of speed and position with time it can be inferred that by applying power system stabilizer the limitation of AVR can be removed.

Plot of Rotor mode Damping ratio and Damping coefficient with exciter gain :

With Power system stabilizer the rotor mode damping ratio and damping coefficient increases with increase in exciter gain, This is as evident from the figure 5.7.

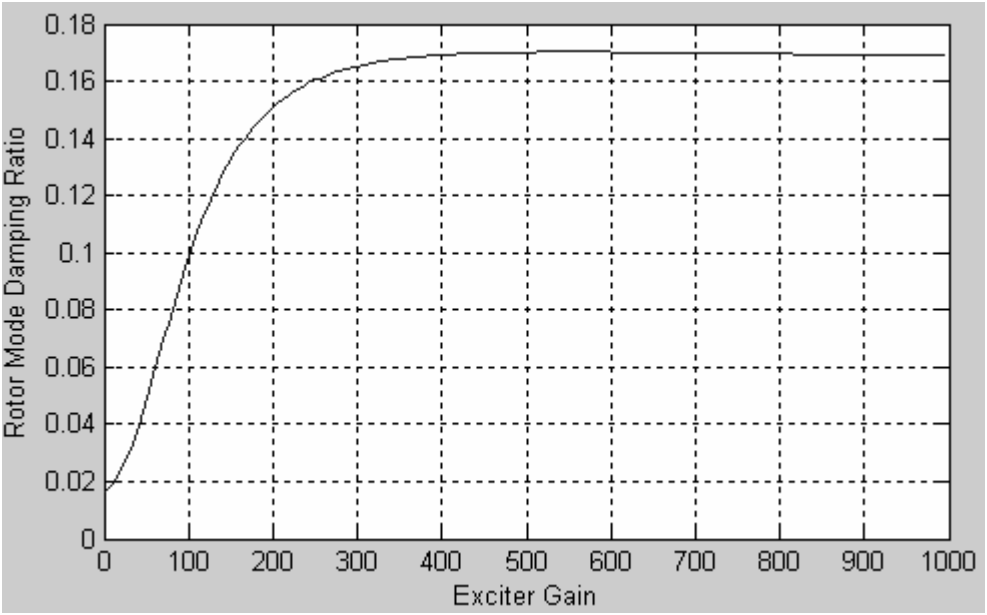

Figure 5.7 Rotor Mode Damping Ratio with Exciter Gain

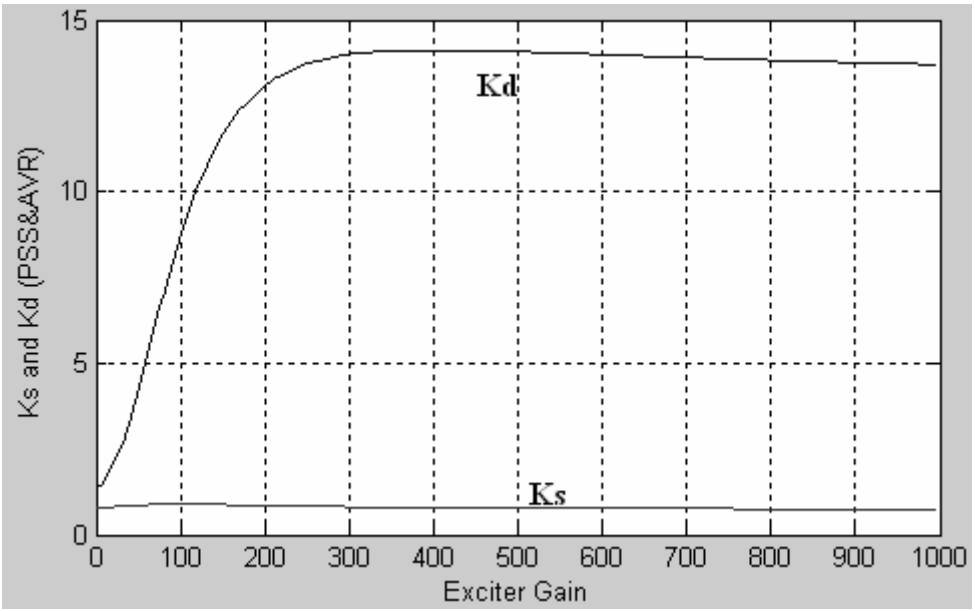

Figure 5.8 Damping and Synchronizing Torque coefficient Vs Exciter Gain for PSS

Figure 5.8 reveals that with increase in exciter gain synchronizing coefficient was positive as before but main variation analyzed by using power system stabilizer was judged in damping torque coefficient which also becomes positive thus providing increased damping to the system.

Next main parameter which is of interest is rotor mode damping ratio 'ζ', now variation of rotor mode damping ratio will be determined when per unit active power deliver by the generator varies over its full range (i.e.0 to 1)

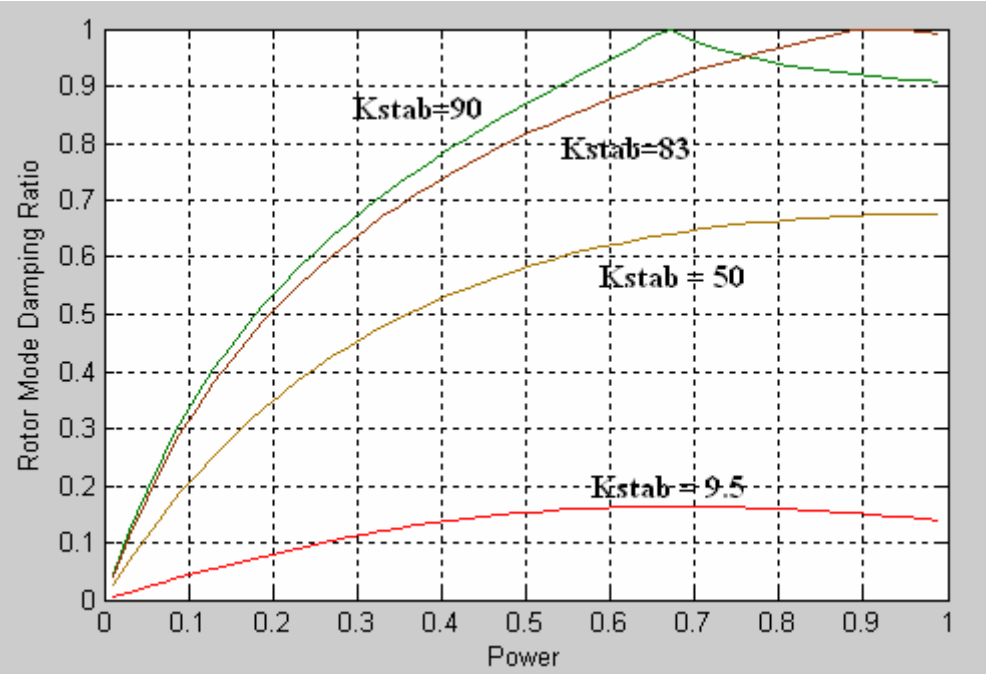

Figure 5.9 Rotor mode damping ratio Vs active power for different K_{STAB}

Above figure demonstrates variation of rotor mode damping ratio for different values of stabilizer gain. The plot depicts that with increase in power for a specific stabilizer gain rotor mode damping ratio keeps on increasing. The maximum value of rotor mode damping ratio achieved depends on the value of stabilizer gain. Damping ratio goes on increasing with the value of stabilizer gain but when it touches unity it bounces back. So will never cross unity, for appropriate damping, requirement of rotor mode damping ratio is unity, this can be done by appropriate selection of stabilizer gain.

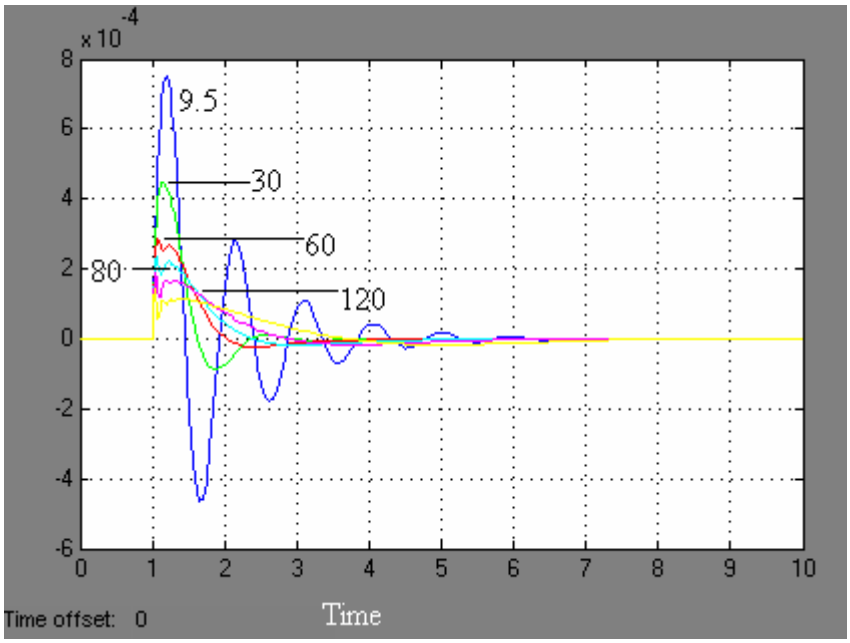

Figure 5.10 Variation of Angular Speed for Different Stabilizer Gain

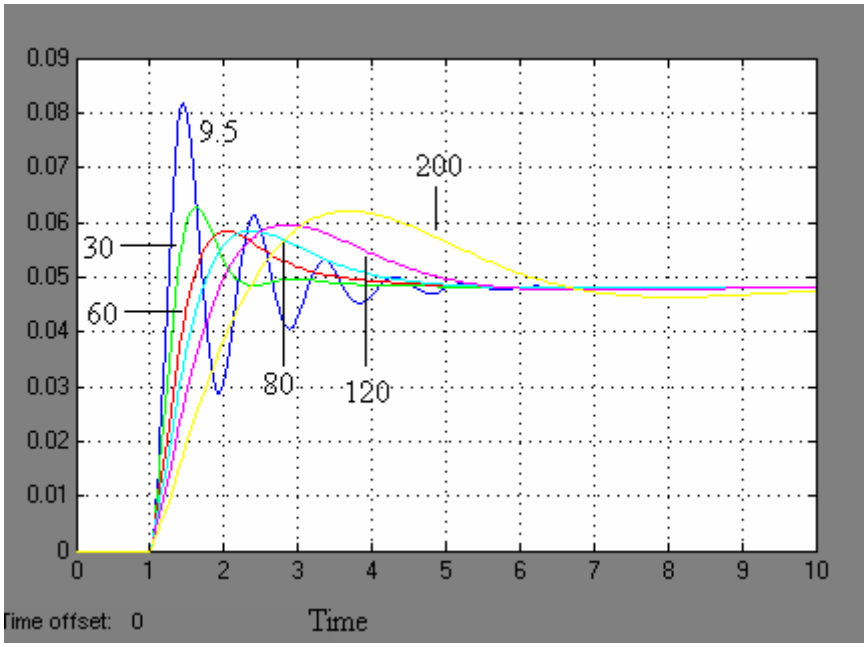

Figure 5.11 Variation of Angular Position for Different Stabilizer Gain

figure 5.10 and 5.11 shows variation in angular speed and angular position for different values of K_{STAB}. These plots characterize the effect of increase in stabilizer gain on Angular position and Angular speed.

As scrutiny of rotor mode damping ratio for fixed stabilizer gain and varying power was carried out. Now variation rotor mode damping ratio with stabilizer gain will be studied for a particular value of active power delivered. The plot is shown below.

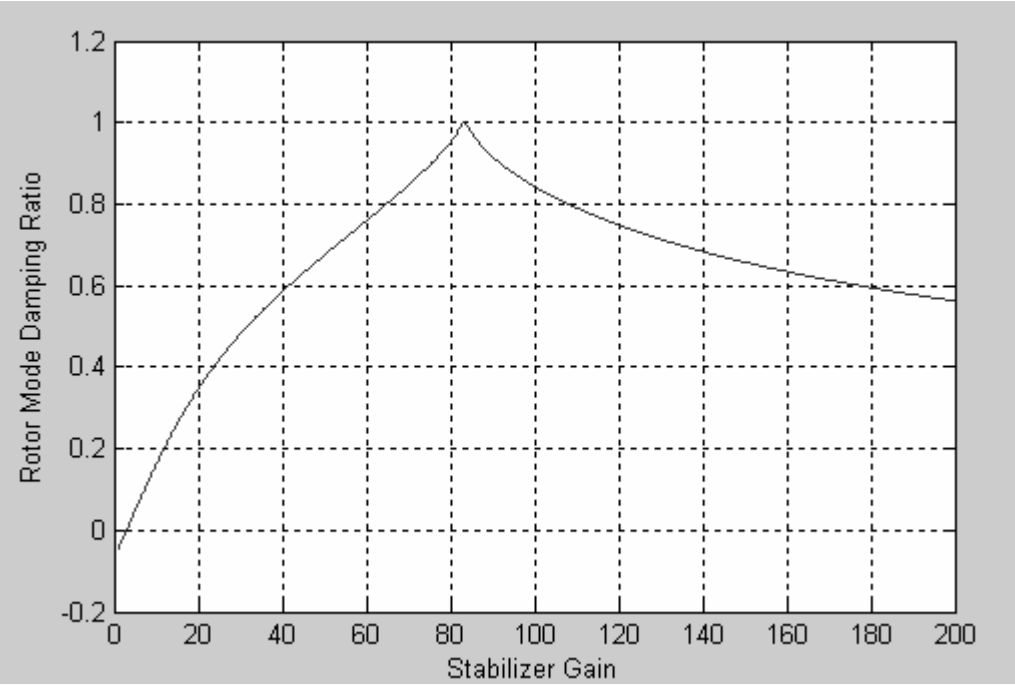

Figure 5.12 Rotor mode damping ratio Vs K_{STAB} for P=0.9 pu

As discussed earlier ideal value of rotor mode damping ratio required for a system is unity. So the main problem faced is finding the value of K_{STAB} which will yield unity rotor mode damping ratio. This problem of selection of stabilizer gain for any constant power can be solved by analyzing the graph and finding the value of K_{STAB} of maximum rotor mode damping ratio. For example in figure 5.12 for per unit active power 0.9 graph is plotted between ζ Vs K_{STAB}. Value of stabilizer gain for maximum power can be identified from the plot which in this case is 83.

Apart from graphical method value of stabilizer gain for maximum damping coefficient can also be found programmatically. This analysis was conceded in discrete domain via a function used for finding Stabilizer Gain.

Plot for the discrete system with parameters same as for block diagram shown in figure 5.13 is shown below.

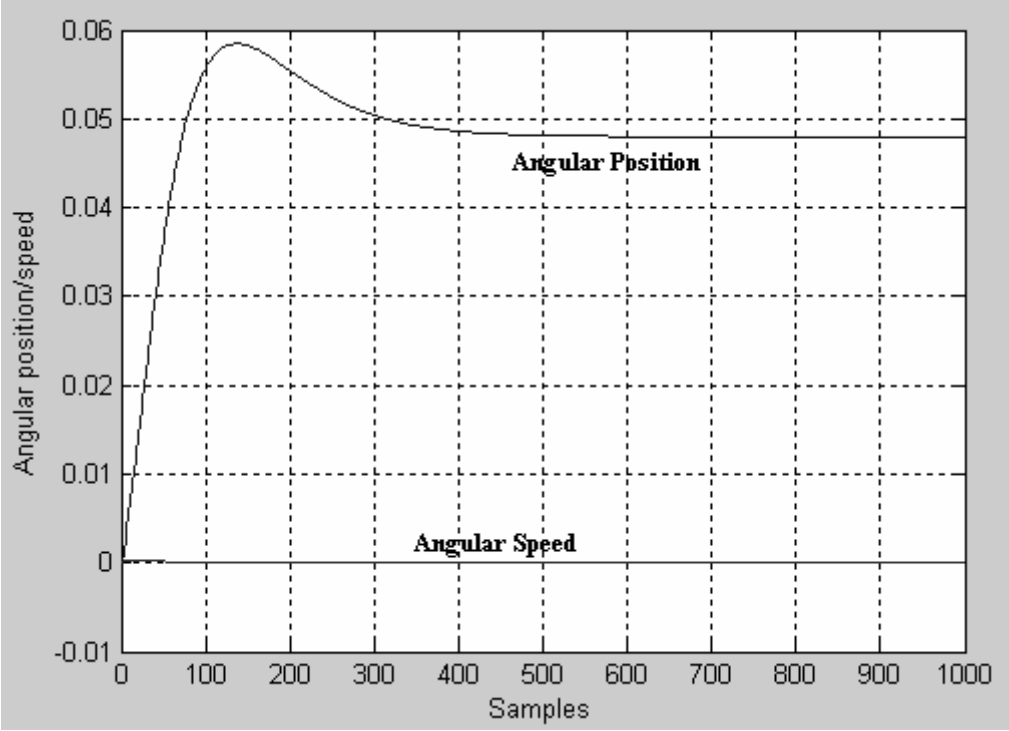

Figure 5.13 plot for discrete system with auto tuned K_{STAB}

Thus with automatic selection of stabilizer gain appropriate damping will be selected for the system that neither generate too much oscillations nor produce sluggish response as publicized in figure 5.13. Similar response can be observed in time domain for similar parameter considerations.

These power system stabilizers suffer from a limitation that they are not proved that much efficient for damping small signal oscillations over wide range for operating conditions. Although the self-tuning PSS has offered better dynamic performance than the fixed-gain PSS, it suffers from a major drawback of requiring model identification in real-time which is very time consuming. Also it requires a deep understanding of a system, exact equations and precise numeric values.

To overcome this problem, a fuzzy logic based power system stabilizer was developed without real-time model identification. The fuzzy logic incorporates an alternative way of thinking which allows one to model complex systems using a higher level of abstraction originated from accumulated knowledge and experience.

Thus next section explains fuzzy logic power system stabilizer, design of fuzzy logic controller and the effectiveness of the FPSS is demonstrated by computer simulation for a single-machine infinite system. To show the superiority of FPSS, its performances are compared with those of conventional power system stabilizer.

CHAPTER 6

FUZZY LOGIC POWER SYSTEM STABILIZER

The method of Power System Stabilizer is designed for using linearized model in the specific operating point show a good control performance in the specific operating point. But these approaches are difficult to obtain a good control performance in case of change in various operating conditions. Therefore fuzzy logic control scheme is used in power system stabilizer to achieve the limitations of previous discussed power system stabilizer this new method is known as fuzzy logic based power system stabilizer. This approach to design power system stabilizer based on two input fuzzy logic controlled is used here for improving small signal stability of the system. The two input are $\Delta\omega$ and $\frac{d}{dt}\Delta\omega$

A fuzzy power system stabilizer (FPSS) is developed using the concept of fuzzy basis functions. The linguistic rules, regarding the dependence of the plant output on the controlling signal, are used to build the FPSS. The FPSS is designed for cogeneration, but simulation studies are based on a one machine-infinite bus model.

6.1 INTRODUCTION TO FUZZY LOGIC

Fuzzy logic is a derivative from classical Boolean logic and implements soft .linguistic variables on a continuous range of truth values to be defined between conventional binary. It can often be considered a suspect of conventional set theory. Since fuzzy logic handles approximate information in a systematic way, it is ideal for controlling non-linear systems and for modeling complex systems where an inexact model exists or systems where ambiguity or vagueness is common. A typical fuzzy system consists of a rule base, membership functions and an inference procedure

FUZZY SUBSETS

In classical set theory, a subset U of asset S can be defined as **a** mapping from the elements of **S** to the elements the subset {0, 1},

U: S → {0.1}

The mapping may be represented as a set of ordered pairs, with exactly one ordered pair present for each element of S. The first element of the ordered pair is an element of the set S, and second element is an element of the set (0, l). The value zero is used to represent non-membership, and the value one is used to represent complete membership. The truth or falsity of the statement 'X is in U' is determined by finding the ordered pair whose first element is X. The statement is true if the second element of the ordered pair is 1, and the statement is false if it is 0.

MERITS OF FUZZY LOGIC

The reasons why fuzzy logic is used are as follows**:**

An alternative design methodology, which is simpler and faster. It reduces the design development cycle. It simplifies design complexity. A better alternative solution to non-linear control. It improves control performance. It is simple to implement. It reduces hardware cost.

6.2 FUZZY LOGIC CONTROLLER

Fuzzy control systems are rule-based systems in which a set of so-called fuzzy rules represent a control decision mechanism to adjust the effects of certain system stimuli. The aim of fuzzy control systems is normally to replace a skilled human operator with a fuzzy rule-based system. The fuzzy logic controller provides an algorithm which can convert the linguistic control strategy based on expert knowledge into an automatic control strategy. Figure 6.1 illustrates the basic configuration of a fuzzy logic controller which consists of a fuzzification interface, a knowledge base, decision making logic, and a defuzzification interface.

The fuzzy controller used in power system stabilizer is normally a two-input and a single-output component. It is usually a MIS0 system. The two inputs are change in angular speed and rate of change of angular speed whereas output of fuzzy logic controller is a voltage signal

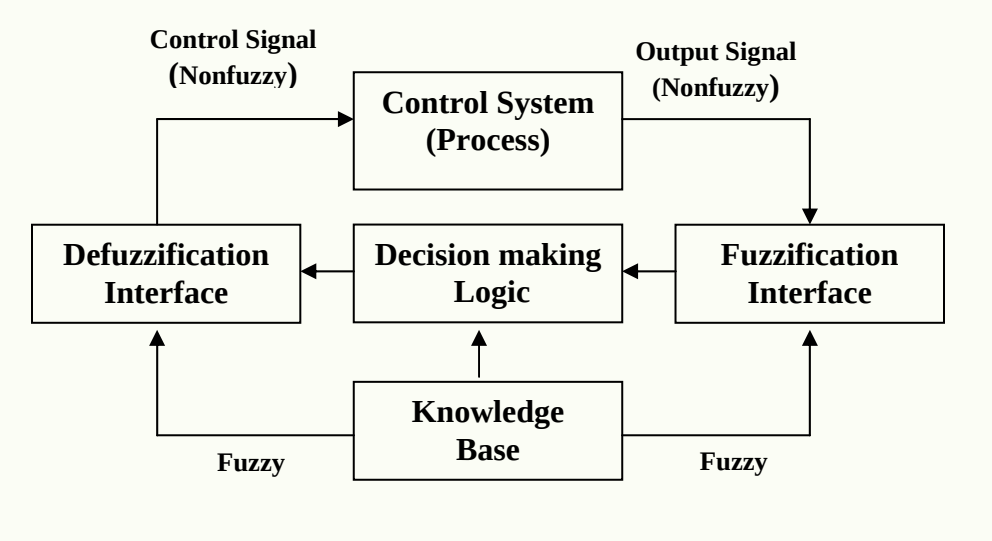

Figure 6.1 The principle Design of fuzzy logic Controller

In fuzzy control, linguistic information from human experts can be placed into two categories:

Fuzzy control rules which set forth the situations in which certain control actions should be taken (e.g., if the speed-deviation is negative medium and the acceleration is negative medium then the PSS output should be negative big).

Fuzzy IF-THEN rules, which describe the behavior of the unknown plant (e.g., if the control signal applied to the synchronous machine is negative, then the acceleration of the shaft will change in a positive direction)

6.3 CONTROLLER DESIGN PROCEDURE

The fuzzy logic controller (FLC) design consists of the following steps .

1) Identification of input and output variables.
2) Construction of control rules.
3) Establishing the approach for describing system state in terms of fuzzy sets, i.e. establishing fuzzification method and fuzzy membership functions.
4) Selection of the compositional rule of inference.
5) Defuzzification method, i.e., transformation of the fuzzy control statement into specific control actions.,

Steps 1 and 2 are application specific and typically straightforward. There are several approaches to Steps 4 and 5 but here we are using center-of-gravity defuzzification procedure.

SELECTION OF INPUT AND OUTPUT VARIABLES:

Define input and control variables, that is, determine which states of the process should be observed and which control actions arc to be considered. For FLPSS design, generator speed deviation $(\Delta\omega)$ and acceleration $(\Delta\dot{\omega})$ can be observed and have been chosen as the input signal of the fuzzy PSS. The dynamic performance of the system could be evaluated by examining the response curve of these two variables.

In practice, only shaft speed $(\Delta\omega)$ is readily available. The acceleration signal $(\Delta\dot{\omega})$ can be derived from the speed signals measured at two successive sampling instants using the following equation:

$$\Delta\dot{\omega}(k) = \frac{((\Delta\omega(k) - \Delta\omega(k-1))}{\Delta T}$$

The control variable is the output from the fuzzy logic controller.

MEMBERSHIP FUNCTION

The linguistic variables chosen for this controller are speed deviation, acceleration and voltage. In this, the speed deviation and acceleration are the input linguistic variables and voltage is the output linguistic variable. The number of linguistic variables varies according to the application. Usually an odd number is used. A reasonable number is seven. However, increasing the number of linguistic variables results in a corresponding increase in the number of rules. Each linguistic variable has its fuzzy membership function. The membership function maps the crisp values into fuzzy variables. The triangular membership functions are used to define the degree of membership. It is important to note that the degree of membership plays an important role in designing a fizzy controller.

Each of the input and output fuzzy variables is assigned seven linguistic fuzzy subsets varying from negative big (NB) to positive big (PB). Each subset is associated with a triangular membership function to form a set of seven membership functions for each fuzzy variable.

NB	Negative Big
NM	Negative Medium

NS	Negative Small
ZE	Zero Error
PS	Positive Small
PM	Positive Medium
PB	Positive Big

Table 6.1 Output and Input Linguistic Variables

First input to the fuzzy controller is acceleration i.e. $(\Delta\dot{\omega})$ it is normalized by multiplying with some factor X_1 so that its value lies between -1 and 1. The membership function for acceleration is shown in figure 6.2.

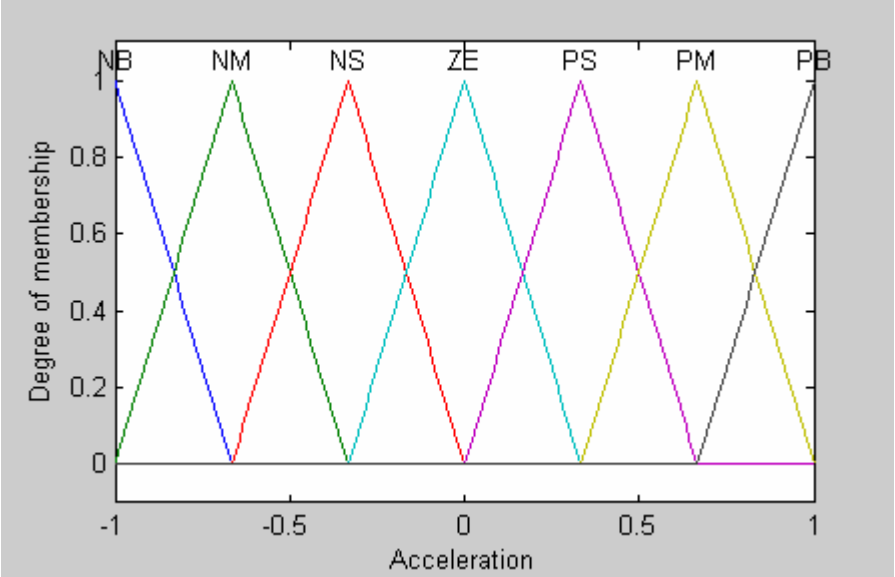

Figure 6.2 Membership Function of Acceleration

Membership function of second input i.e. Speed deviation $(\Delta\omega)$ also has same membership function that of acceleration and with 50% overlap between adjacent fuzzy subsets, the function is shown in figure below.

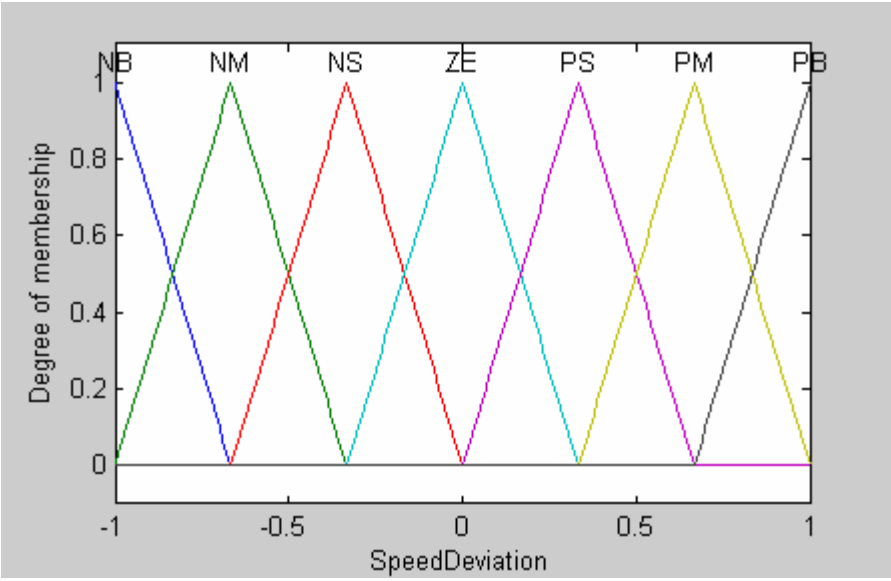

Figure 6.3 Membership Function of Speed Deviation

There is only one output from the fuzzy logic controller i.e. voltage signal (Vs) its membership function also contains seven subsets as defined in table 6.1 with 50% overlap the only difference is that we have to renormalized the output by multiplying the output from fuzzy controller with a constant gain X_3. The membership function of voltage signal is shown in figure 6.4.

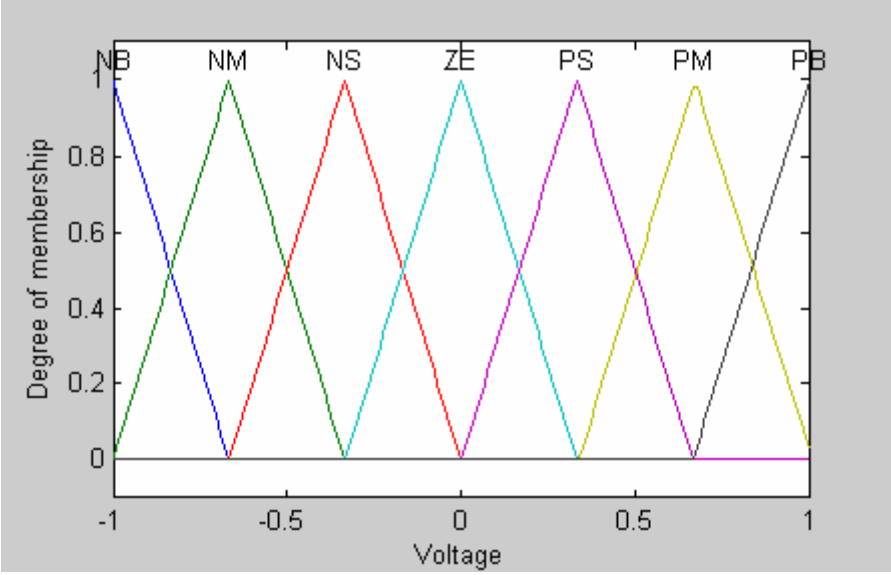

Figure 6.4 Membership function of output Voltage signal.

FUZZY RULE BASE

A set of rules which define the relation between the input and output of fuzzy controller can be found using the available knowledge in the area of designing PSS. These rules are defined using the linguistic variables. The two inputs, speed and acceleration, result in 49 rules for each machine. A proper way to show these rules is given in Table 6.2 where all the symbols are defined in the basic fuzzy logic terminology. A typical rule has the following structure:

Rule 1: If speed deviation is LP (large positive) AND acceleration is LN (large negative) then FPSS (output of fuzzy PSS) is VS (very small).

Similarly all 49 rules can be explained using the table.

$\Delta\dot{\omega}$ / $\Delta\omega$	**NB**	**NM**	**NS**	**ZE**	**PS**	**PM**	**PB**
NB	NB	NB	NB	NB	NM	NM	NS
NM	NB	NM	NM	NM	NS	NS	ZE
NS	NM	NM	NS	NS	ZE	ZE	PS
ZE	NM	NS	NS	ZE	PS	PS	PM
PS	NS	ZE	ZE	PS	PS	PM	PM
PM	ZE	PS	PS	PM	PM	PM	PB
PB	PS	PM	PM	PB	PB	PB	PB

Table 6.2 Decision Table for fuzzy logic controller

The stabilizer output is obtained by applying a particular rule expressed in the form of membership functions. There are different methods for finding the output in which Minimum-Maximum and Maximum Product Method are among the most important ones. Here, the Min-Max method is used. Finally the output membership function of the rule is calculated. This procedure is carried out for all of the rules and every rule an output membership function is obtained.

Using min-max inference, the activation of the ith rule consequent is a scalar value (Vs) which equals the minimum of the two antecedent conjuncts' values. For example if $\Delta\omega$ belongs to NB with a membership of 0.3 and $\Delta\dot{\omega}$ belongs to NM with a membership of 0.7 then the rule consequence i.e. Voltage signal (Vs) will be 0.3.

The knowledge required to generate the fuzzy rules can be derived from an offline simulation. Some knowledge can be based on the understanding of the behavior of the dynamic system under control. However, it has been noticed in practice that, for monotonic

systems, a symmetrical rule table is very appropriate, although sometimes it may need slight adjustment based on the behavior of the specific system. If the system dynamics are not known or are highly nonlinear, trial-and-error procedures and experience play an important role in defining the rules.

DEFUZZIFICATION

The input for the defuzzification process is a fuzzy set (the aggregate output fuzzy set) and the output is a single number. As much as fuzziness helps the rule evaluation during the intermediate steps, the final desired output for each variable is generally a single number. However, the aggregate of a fuzzy set encompasses a range of output values, and so must be defuzzified in order to resolve a single output value from the set.

Perhaps the most popular defuzzification method is the centroid calculation, which returns the center of area under the curve. There are five other methods: centroid, bisector, middle of maximum (the average of the maximum value of the output set), largest of maximum, and smallest of maximum. Here in fuzzy logic controller centriod method of defuzzification was opted.

For a discretised output universe of discourse

$\boldsymbol{Y = \{ y_1, \ldots, y_p \}}$

Which gives the discrete fuzzy centroid, the output of the controller is given by following expression:

$$u_k = \frac{\sum_{i=1}^{p} y_i w_i}{\sum_{i=1}^{p} w_i}$$

6.3 IMPLEMENTATION OF FUZZY LOGIC

Block diagram representation of fuzzy logic controller implemented on single machine infinite bus system is shown in the figure below.

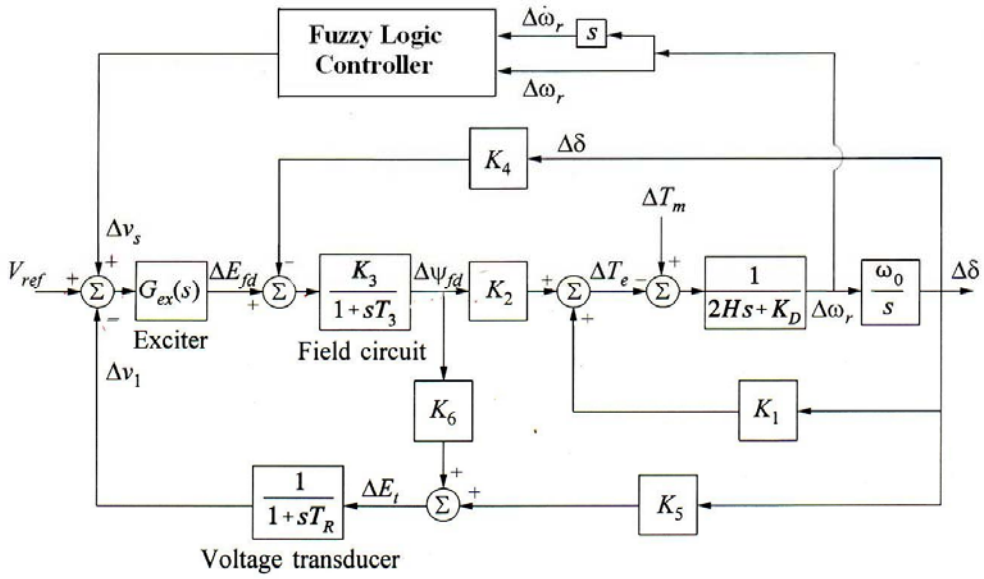

Figure 6.5 Block diagram representation with Fuzzy Logic Controller

The only difference in application of fuzzy logic to single machine infinite bus and conventional power system stabilizer is that in former case the PSS block is replaced by the fuzzy logic controller block. In case of fuzzy implementation, the output control signal Δv_S depends on the change of angular speed and rate of change of angular speed but in case of PSS the control signal Δv_S is function of change of angular speed. Therefore the FPSS will be more effective in damping of small signal oscillation as compared to conventional PSS. Response of fuzzy logic controller depends on various parameters but among all the parameters the most effective are the scaling factor of input and output variables. These are

the two type of parameters whose selection has a significant effect on the output of fuzzy logic controller. Their explanation follows next

The fuzzy module has two inputs, the angular velocity $\Delta\omega$ and its derivative i.e. angular acceleration $\Delta\dot{\omega}$. These are scaled by two coefficients, respectively K_{in1} and K_{in2}, in order to match the range on which the membership functions are defined. Seven triangular membership functions are defined for each input and output that is scaled by a coefficient K_{out}. The main problem that was faced now is the tuning of these fuzzy logic parameters. These parameters were tuned using the following simple procedure.

Initially set the value of K_{in2} and K_{out} equal to unity and study the effect of variation of third parameter on the response of the system and among them select the most suitable value then vary other variables keeping two parameter constant. Follow this procedure to investigate the effect of all three constants on the system. Then after studying the effect of these parameters on system, suitable selection can be made following the similar procedure until we get the desired response.

Previous experience with the controlled system is helpful in selecting the initial value of the FLC parameters. If sufficient information is not available about the controlled system, FLC parameters can become a tedious trial-and-error process.

The main problem faced in fuzzy logic is the tuning of these scaling parameters. Manual tuning was employed initially where previous experience with the controlled system is helpful in selecting the initial value of the fuzzy logic controller parameters. But if sufficient information is not available about the controlled system, then the tuning of these scaling is somewhat tedious task, so genetic based learning procedure can be used for the tuning of tuning of these parameter, described in detail in next chapter.

CHAPTER 7

GENETIC ALGORITHM

The identification of parameters in a fuzzy model can be viewed as an optimization problem, finding parameter values that optimize the model based on given evaluation criteria. Therefore, search and optimization techniques can be applied to parameter identification as well. This chapter introduces one of those optimization techniques - genetic algorithms

7.1 BASICS OF GENETIC ALGORITHM

Genetic Algorithms (GA) are global search and optimization techniques modeled from natural genetics, exploring search space by incorporating a set of candidate solutions in. parallel. A Genetic Algorithm (GA) maintains a population of candidate solutions where each candidate solution is usually coded as a binary string called a chromosome. A chromosome, also referred to as a genotype, encodes a parameter set for a set of variables being optimized. Each encoded parameter in a chromosome is called a gene. A decoded parameter set is called a phenotype. A set of chromosomes forms a population, which is evaluated and ranked by a fitness evaluation function. The fitness evaluation function plays a critical role in GA because it provides information about how good each candidate solution is. This information guides the search of a genetic algorithm. More accurately, the fitness evaluation results determine the likelihood that a candidate solution is selected to

produce candidate solutions in the next generation. The initial population is usually generated at random.

The evolution from one generation to the next one involves mainly three steps: (1) fitness evaluation, (2) selection, and (3) reproduction.

First, the current population is evaluated using the fitness evaluation function and then ranked based on their fitness values. Second, GA stochastically select "parents" from the current population with a bias that better chromosomes are more likely to be selected. This is accomplished using a selection probability that is determined by the fitness value or the ranking of a chromosome,. Third, the GA reproduces “children” from selected "parents" using two genetic operations*:* crossover and mutation. This cycle of evaluation, selection, and reproduction terminates when an acceptable solution is found when a convergence criterion is met, or when a predetermined limit on the number of iterations is reached. The crossover operation produces offspring by exchanging information between two parent chromosomes. The mutation operation produces an offspring from a parent through a random modification of the parent. The chances that these two operations apply to a chromosome are controlled by two probabilities: the crossover probability and the mutation probability typically, the mutation operation has a low probability of reducing its potential interference with a legitimately progressing search.

7.2 DISTINCTION FROM OTHER TECHNIQUES

GA are exploratory search and optimization procedures that were devised on the principles of natural evolution and population genetics. Unlike other optimization techniques, GA work with a population of individuals represented by bit strings and modify the population with random search and competition. The advantages of GA over other traditional optimization techniques can be summarized as follows:

- GA work on a coding of the parameters to be optimized, rather than the parameters themselves.
- GA search the problem space using a population of trials representing possible solutions to the problem, not a single point, i.e. GA has implicit parallelism. This property ensures GA to be less susceptible to getting trapped on local minima.
- GA uses a performance index assessment to guide the search in the problem space.
- GA use probabilistic rules to make decisions.

7.3 TUNING OF PSS PARAMETERS

Applying the GA to the problem of PSS design involves performing the following two steps.

- The performance index value must be calculated for each of the strings in the current population. To do this, the tuning parameters must be decoded from each string in the population and the system is simulated to obtain the performance index value.
- GA operations are applied to produce the next generation of the strings.

These two steps are repeated from generation to generation until the population has converged producing an optimal or near optimal parameter set.

Tuning of the three scaling parameter was done offline using genetic algorithm. Then these parameters were placed in the fuzzy logic controlled and required response was obtained. The objective of the offline tuning algorithm used here is to change the controller gains to obtain the desired system response. The tuning algorithm tries to optimize three system performance indices to minimize the fitness function. Results of genetic algorithm were mainly governed by the fitness evaluation function. Applying the GA to the problem of PSS design involves performing the following two steps.

- The performance index value must be calculated for each of the strings in the current population. To do this, the tuning parameters must be decoded from each string in the population and the system is simulated to obtain the performance index value.
- GA operations are applied to produce the next generation of the strings.

These two steps are repeated from generation to generation until the population has converged producing an optimal or near optimal parameter set.

Tuning of the three scaling parameter was done offline using genetic algorithm. Then these parameters were placed in the fuzzy logic controlled and required response was obtained. The objective of the offline tuning algorithm used here is to change the controller gains to obtain the desired system response. The tuning algorithm tries to optimize three system performance indices to minimize the fitness function. Results of genetic algorithm were mainly governed by the fitness evaluation function.

A good design of fitness evaluation function is probably the most important factor in a successful application of GA. However, its, importance can be easily overlooked. When a GA does performs well in solving an optimization problem, a natural temptation is a change a GA design parameter (e.g., the population size, the crossover probability, or dot mutation probability). Even though changing these parameters does affect the performance of GA, tuning GA parameters will be in vain if the, fitness evaluation function does not correctly reflect the desired optimization criteria.

A fitness-based function calculates how well a model using the parameter set in a chromosome fits a set of input-output training data. In other words, the function computes the error between the target's output and the model's output. A performance-based evaluation function determines how well a system using the parameter set in a chromosome achieves a set of performance objective.

CHAPTER 8

SIMULATION RESULTS

Model used in Simulink/ Matlab to analyze the effect of fuzzy logic controller in damping small signal oscillations when implemented on single machine infinite bus system is shown below in figure 5.3.

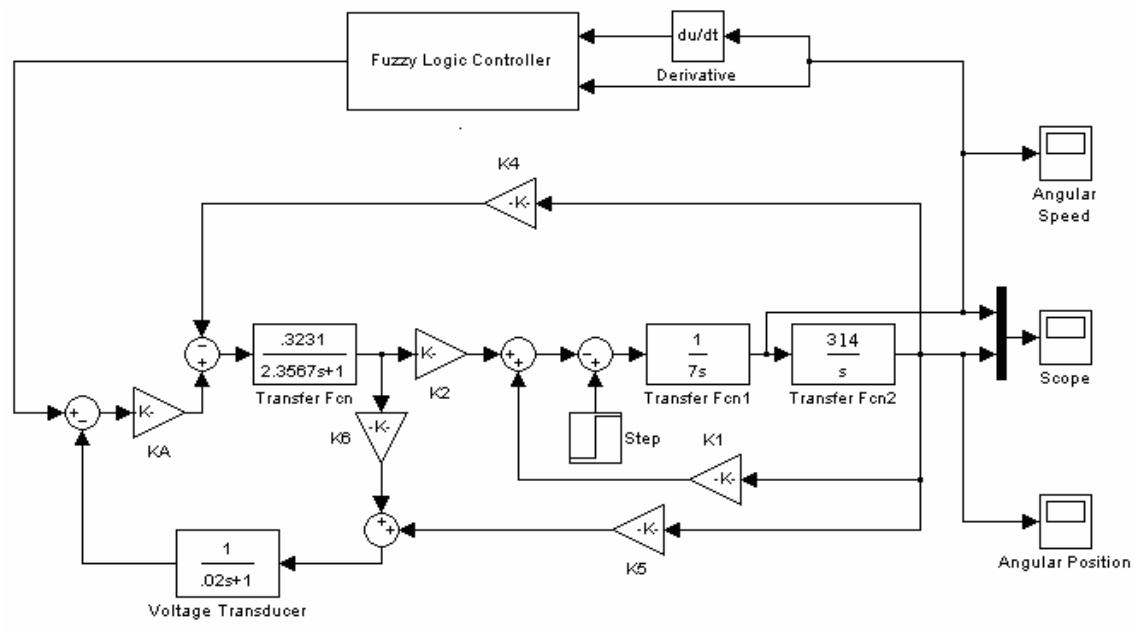

Figure 8.1 Simulink Model with Fuzzy Logic Controller

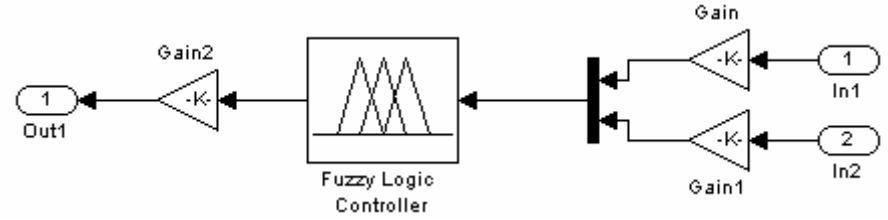

Figure 8.2 Expanded form of Fuzzy logic controller block

The fuzzy logic controller block consists of fuzzy logic block and two type of scaling factors. One is input scaling factors, these are two in number one for each input as the other is output scaling factor which determine the extent to which controlling effect is produced by the controller

8.1 FUZZY INFERENCE SYSTEM

Fuzzy logic block is prepared using fis file in Matlab 7 command prompt or by fuzzy logic tool box . Plot of the fis file is as shown in figure 8.3.

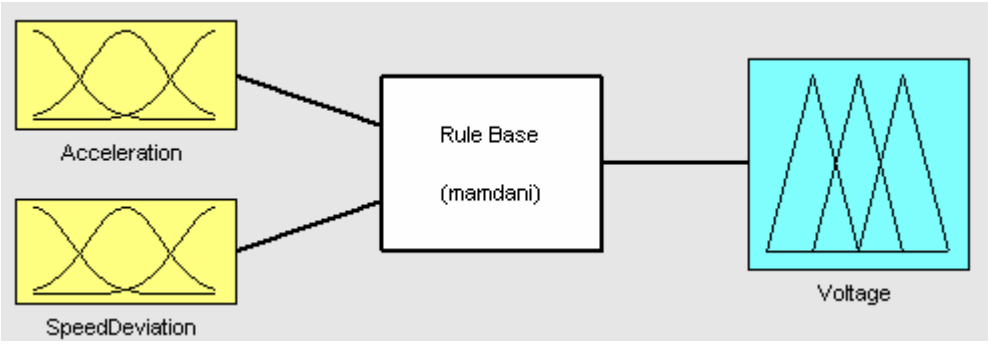

Figure 8.3 Plot of fuzzy logic controller prepared using matlab

The above fuzzy system is implemented using following FIS (fuzzy Inference System) properties:

And Method: Min

Or Method: Max

Implication: Min

Aggregation: Max

Defuzzyfication: Centroid

For the above FIS system Mamdani type of rule-base model is used. This produces output in fuzzified form. Normal system need to produce precise output use a defuzzification process to convert the inferred possibility distribution of an output variable to a representative precise value. In the given fuzzy inference system this work is done using centroid defuzzyfication principle. In the system clipping inference method (i.e. the min implication) is used together with the max aggregation operator.

Given FIS is having seven input member function for both input variables leading to 7*7 i.e. 49 rules. Figure 8.4 shows these rules using rule viewer.

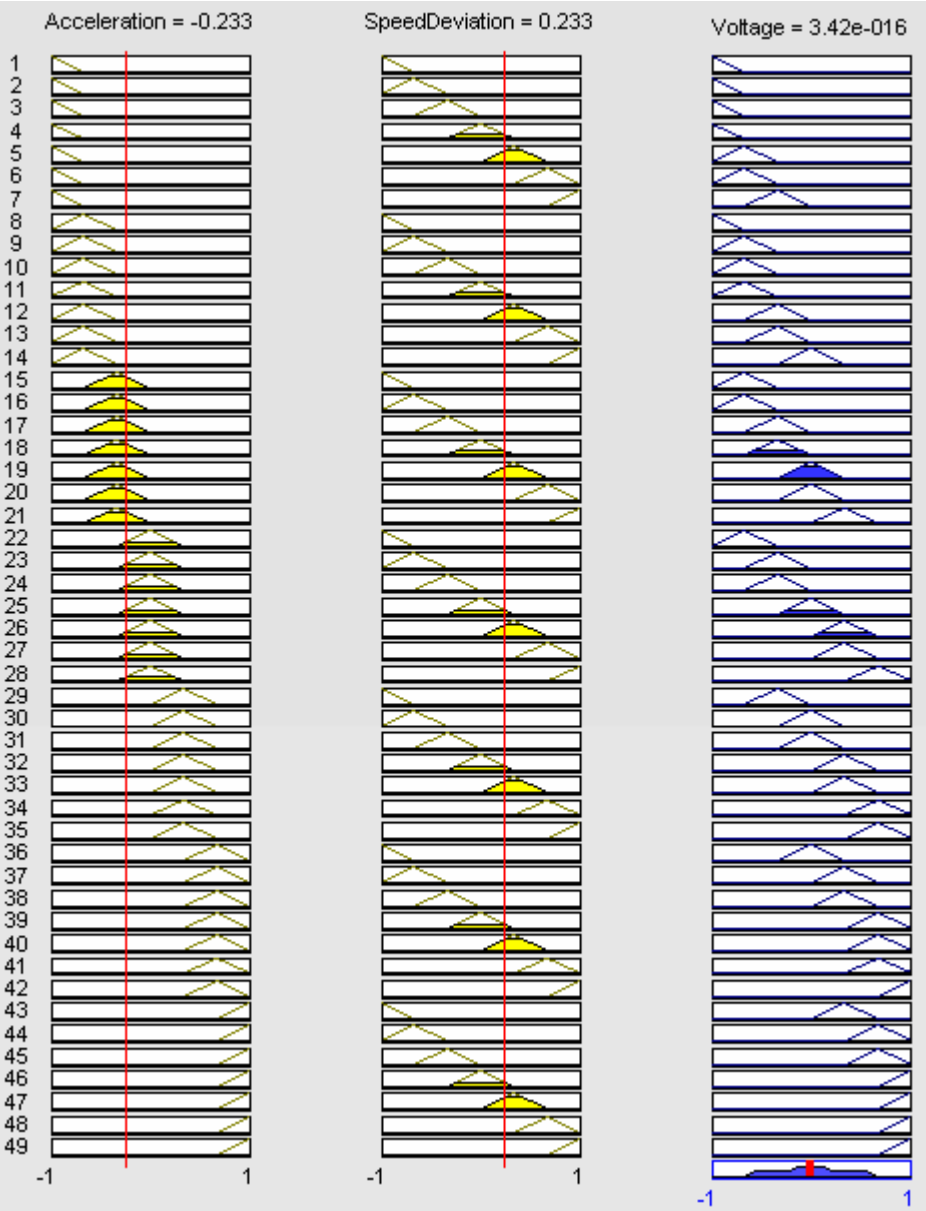

Figure 8.4 Rule viewer for the Fuzzy inference system

The Rule Viewer displays a roadmap of the whole fuzzy inference process. The first two columns of plots show the membership functions referenced by the antecedent, or the if-part of each rule. The third column of plots shows the membership functions referenced

by the consequent, or the then-part of each rule. Yellow colour in first two plots represents the antecedent rules fired for a particular value and blue colour in third column represents the consequence of the antecedent on the output. Blue colour line in the last block of third column represents the final precise value calculated using centroid defuzzification method.

The Rule Viewer shows one calculation at a time and in great detail. In this sense, it presents a sort of micro view of the fuzzy inference system. If the entire output surface of system is to be viewed, that is, the entire span of the output set based on the entire span of the input set, The Surface Viewer is required. Figure 8.5 show the surface view of the system under consideration.

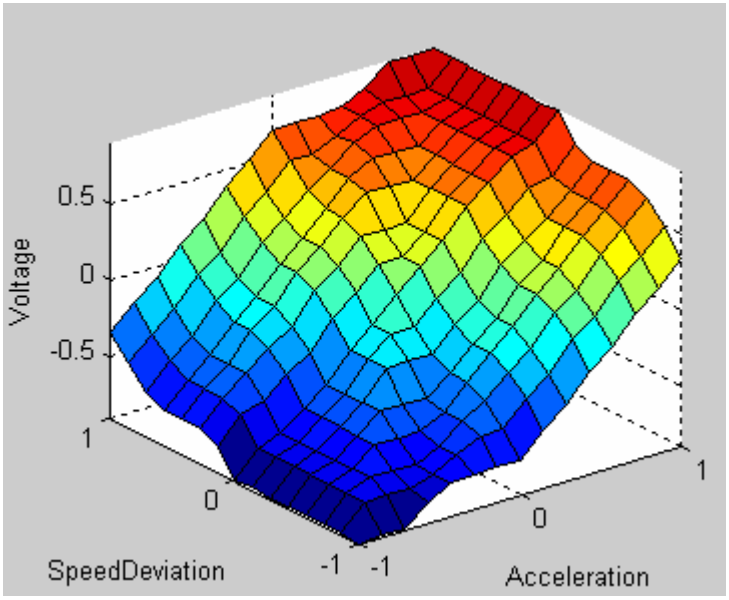

Figure 8.5 Surface viewer for FIS

The Surface Viewer has a special capability that is very helpful in cases with two (or more) inputs and one output: you can actually grab the axes and reposition them to get a different three-dimensional view on the data.

8.2 RESULTS WITH FUZZY LOGIC

Using fuzzy logic power system stabilizer it can inferred that it does not require any complex mathematical calculations and the response with fuzzy logic is much improved than with conventional power system stabilizer. It is illustrated using the plots of angular speed and angular acceleration shown in figure 8.5 and 8.6.

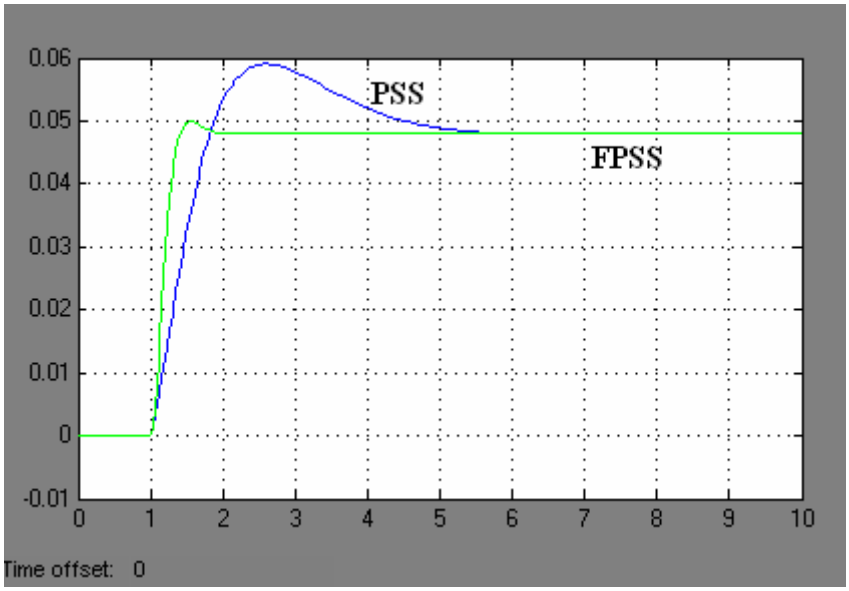

Figure 8.6 Variation of Angular position with time for PSS and FPSS

Figure 8.6 shows the relative plots for variation of angular position with time for PSS and FPSS. These results are for 5% change in mechanical torque. From figure it can be perceived that with the application of fuzzy logic the rise time and the settling time of the system decreases also there is significant decrease in the peak overshoot of the system. The system reaches its steady state value much earlier with fuzzy logic power system stabilizer compared to conventional power sytem stabilizer.

Figure 8.7 shows the relative variation of angular position with time for PSS and FPSS.

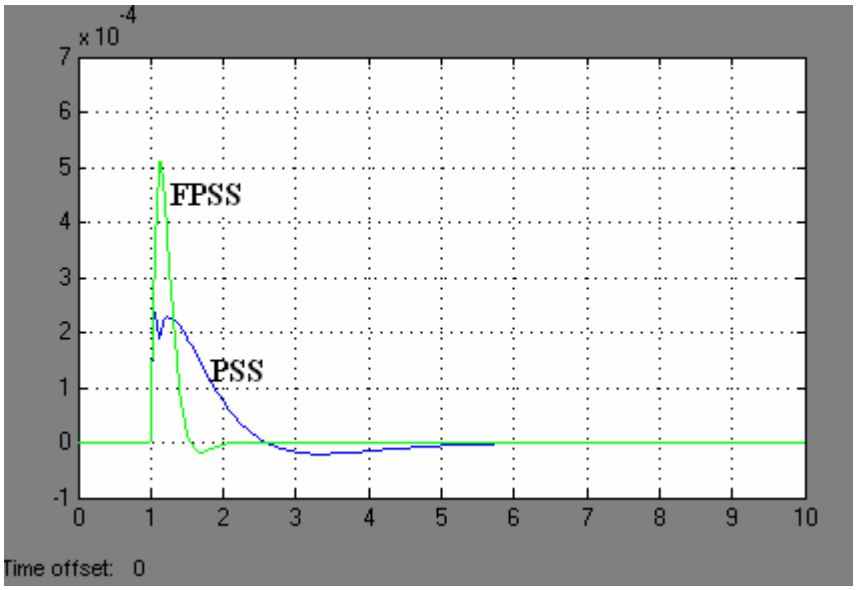

Figure 8.7 Variation of Angular speed with time for PSS and FPSS

From relative plots it can be retrieved that oscillations in angular speed reduces much faster with fuzzy logic power system stabilizer than with conventional power system stabilizer. As shown in figure with fuzzy logic the variation in angular speed reduces to zero in about 2 seconds, but with conventional power system stabilizer it takes about 6 seconds to reach to final steady state value.

Figure 8.6 and 8.7 for fuzzy logic are drawn by selecting following values for the three scaling factors.

$$Kin1 = 1.6$$
$$Kin2 = 29.56$$
$$Kout = 1.06$$

The effect of genetic algorithm will be analyzed next on fuzzy logic controller and finally on fuzzy logic power system stabilizer.

8.3 RESULTS WITH GFPSS

GFPSS signifies fuzzy logic controller parameters tuned using genetic algorithm. The parameters which are tuned are the scaling factors. This is an offline tuning procedure. For tuning these parameters one fitness function is to be designed. Then optimum values of these parameters are determined using genetic algorithm, these optimum values are then substituted in the system to get the final response. The fitness function used in this case is the sum of the square of deviation of angular position from the steady state value. Here steady state value of angular position was found without applying genetic algorithm. The fitness function in mathematical form is:

$$J = \sum_{i=1}^{n} (\delta_{SteadyState} - \delta_i)^2$$

Where

δ_i is the angular position for i^{th} iteration, and 'i' varies from 1 to n.

This function J is then to be minimized using genetic algorithm. After minimizing the function using genetic algorithm following results are obtained.

Best Fitness function value 0.070793

Mean Fitness function value 0.07499

Values of Scaling Parameters:

Kin1 0.55894

Kin2 12.83679

Kout 2.22694

Applying the parameters calculated by genetic algorithm.

Using these parameters performance of the proposed fuzzy logic based power system stabilizer tuned through genetic algorithm, compared with fuzzy logic power system stabilizer, for 5% step increase in mechanical torque Tm is shown in figure 8.8 and 8.9 for variation in angular position and angular speed.

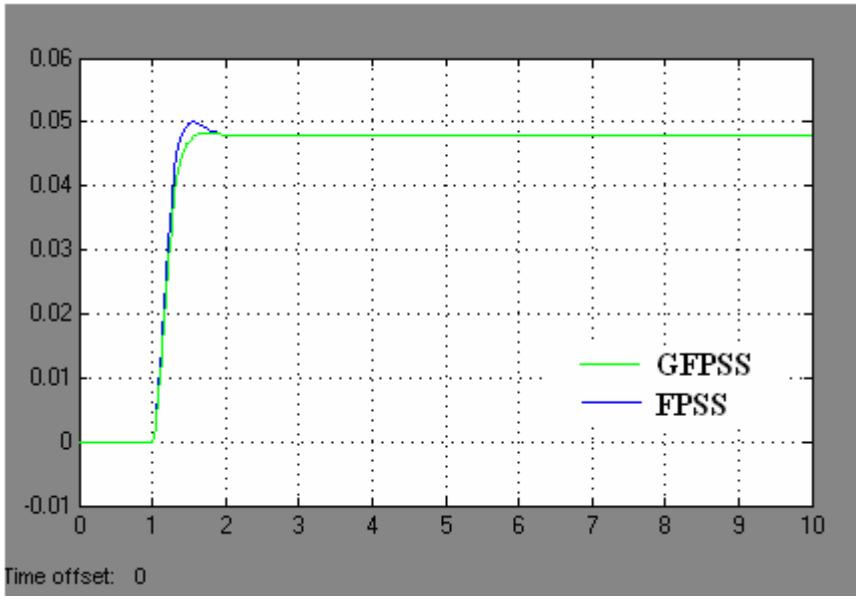

Figure 8.8 Variation of angular Position with time for GFPSS and FPSS

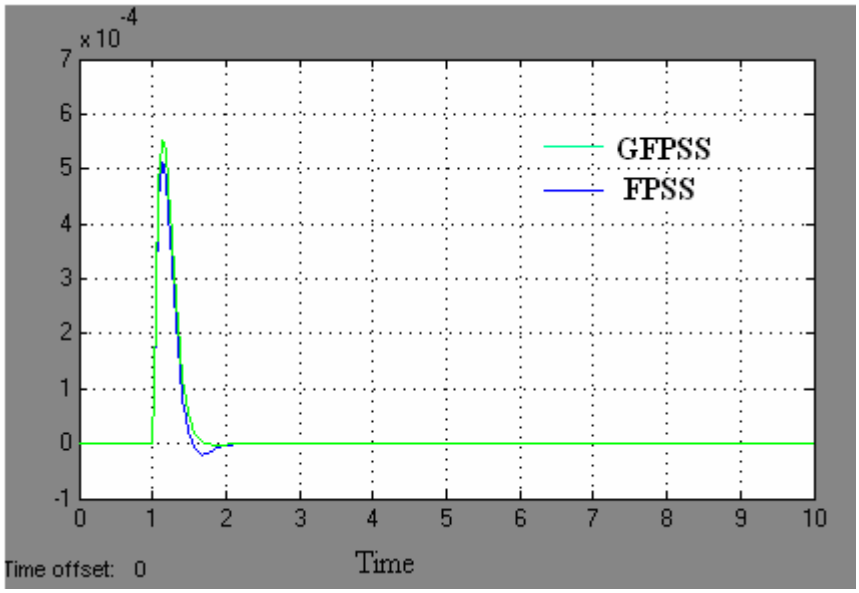

Figure 8.9 Variation of angular speed with time for GFPSS and FPSS

Results in figure 8.8 and 8.9 are for 5% change in mechanical torque. The variation of angular speed and position depicts that by tuning of fuzzy logic controller parameters using genetic algorithm, an improved response is obtained. The overshoot and settling time for the variation in angular position decrease with the application of genetic algorithm. Although the improvement is small, GAFPSS proved to be more effective in tuning of fuzzy logic parameters and hence damping of small signal oscillations.

Relative comparison of PSS, FPSS and GFPSS for variation in angular position is shown in figure 8.10.

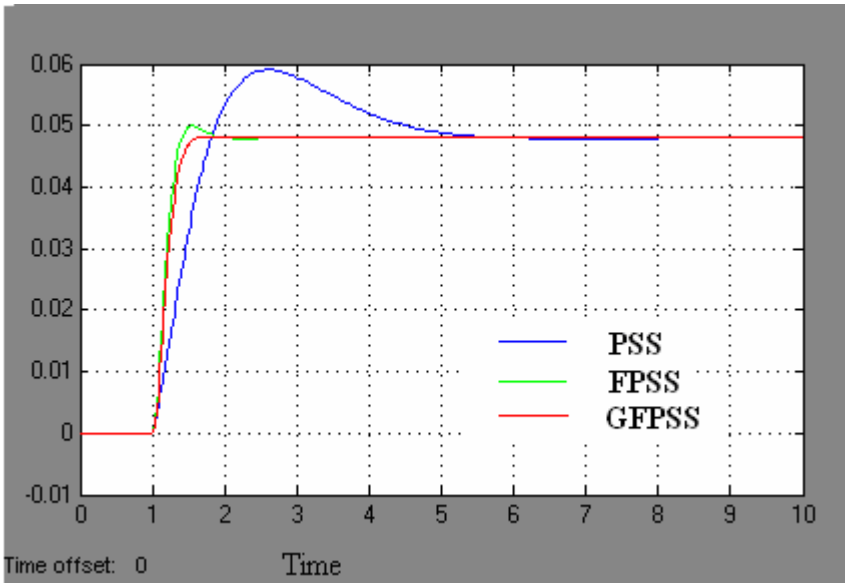

Figure 8.10 Comparative plot for PSS, FPSS and GFPSS

Comparative study reveals that genetic tuned power system stabilizer (GFPSS) is having best performance results. Therefore genetic tuned fuzzy logic power system stabilizer is much more effective than other techniques in damping of power system oscillations.

CONCLUSION AND FUTURE SCOPE OF WORK

In this thesis work initially the effectiveness of power system stabilizer in damping power system stabilizer was reviewed then fuzzy logic power system stabilizer was introduced Speed deviation $\Delta\omega$ and acceleration $\Delta\dot{\omega}$ of synchronous generator were taken as the input signals to the fuzzy controllers.

FPSS shows the better control performance than power system stabilizer in terms of settling time and damping effect. The proposed FPSS produces better damping effect than PSS. To further increase the stability of the power system a technique was introduced to tune parameters of fuzzy logic controller. This technique which performs effective tuning of controller parameters is genetic algorithm. This GAFPSS was designed by incorporating genetic algorithm to search for the optimal settings of FPSS tuning parameters, this tuning was done offline. It is thus possible to realize the controller efficiently and quickly. Lack of online complicated mathematical computations makes it more reliable for real-time applications where small signal stability is required. Using genetic algorithm for tuning of the parameters the best possible FLC was designed Simulation results show that the proposed controller gives better small signal stability over the Conventional PSS. The proposed GFPSS provides good damping characteristics during small signal oscillations. In addition, the coordination between the proposed GFPSS and the conventional stabilizers was also demonstrated.

In the end it can be concluded that the performance of the proposed FPSS is much better and the oscillations are damped out much quicker.

Here genetic algorithm was introduced to tune the parameters of fuzzy logic. It is worth noting that all simulations above were carried out using the proposed FPSS with the tuning parameters optimized by genetic algorithm. This indicates that

although the proposed GPSS parameters are optimized at a single operating point, it can provide good damping to the system oscillations over a wide range of operating conditions.

The tuning was performed offline. Only three scaling factors are tuned using genetic algorithm and proved very much effective in damping small signal oscillations. In addition to scaling factors other parameter can be selected for the tuning and other techniques can be applied for the purpose in conjunction with genetic algorithm. These parameters may include the parameters of membership function, type of membership function etc. In present work offline tuning procedure was applied which was proved effective. But if tuning will be done online than it may improve the performance of the system to a greater extent.

REFERENCES:

[1] Recommended Practice for Excitation System Models for Power System Stability Studies," IEEE Standard 421.5-1992, August 1992.

[2] E.V. Larsen and D.A. Swann. "Applying Power System Stabilizers Part I: General Concept " IEEE Transactions on Power Apparatus and Systems, vol. PAS-100, no 6,June 1981, pp. 3017-3024.

[3] John Yen and Reza Langari "Fuzzy Logic Intelligent Control and Information" Pearson Education Publishing Company.

[4] Minimum/Maximum excitation limiter performance goals for small generation. T.W. Eberly and R.C. Schaefer. IEEE Trans. Energy Conversation, vol. 10, pp.714-721, Dec. 1995

[5] F.P. Demello and C. Concordia, "Concepts of Synchronous Machine Stability as Affected by Excitation Control," IEEE Transactions on Power Apparatus and Systems, vol. PAS-88, No. 4, pp. 316-329, April 1969.

[6] M. Klein, G.J.Rogus and P.Kundur, "A Fundamental Study of Inter-Area Oscillations," IEEE Trans., pp. 914-921, August 1991.

[7] Michael J. Basler and Richard C. Schaefer "Understanding Power System Stabilizer," Basler Electric Company IEEE Trans., pp. 46-67, August 2005.

[8] M.L. Kothari, J. Nanda, and K. Bhattacharya, "Design of Variable Structure Power System Stabilizers with Desired Eigen values in the Sliding Mode," IEE Proceedings, Part C,vol. 140, No.4, July 1993.

[9] M. Jamshidi, N. Vadiee, and T. Ross, Fuzzy Logic and Control, Prentice Hall, 1993.

[10] T. Hiyama and C.M. Lim, ”Application of Fuzzy Logic Control Scheme for Stability Enhancement of a Power System,” IFAC Intemational Symposium on Power Systems and Power Plant Control, Seoul, Korea, pp. 3 13-3 16, 1989.

[11] P Kundur, **“**POWER SYSTEM STABILITY AND CONTROL**”,** McGraw-Hill, 1994.

[12] T. Hiyama and C.M. Lim,”Application of Fuzzy Logic Control Scheme for Stability Enhancement of a Power System,” IFAC Intemational Symposium on Power Systems and Power Plant Control, Seoul, Korea, pp. 3 13-3 16, 1989.

[13] Timothy J.Rose, “FUZZY LOGIC WITH ENGINEERING APPLICATIONS, Mc – Graw Hill.Inc, Newyork, 1997.

[14] EL-METWALLY, K.A., and MALIK, O.P.: ‘Parameter tuning for fuzzy logic controller’. Proceedings IFAC 12th World Congress on Automatic Control, Sydney, Australia, Vol. 2, July 1993, pp. 581-584

[15] Recommended Practice for Excitation System Models for Power System Stability Studies," IEEE Standard 421.5-1992, August 1992.

[16] BRAAE, M., and RUTHERFORD, D.A.: ‘Selection of parameters for a fuzzy logic controller’, Fuzzy Sets and Systems, 1979, 2, pp. 185-199

[17] K.Tomsovic, ”Fuzzy systems applications to power systems”, IEEE PES Tutorial, july2000.

[18] Y. L. Abdel-Magid and M. M. Dawoud," Genetic algorithms applications in load frequency control," Conference of Genetic Algorithms in Engineering Systems: Innovations and Applications, Sept. 1995.

[19] D.E Goldberg, Genetic algorithms in searcl1,optiniization and machme learning' Addison-wesley, Reading, MA, 1989.